International Geology Review, Vol. 47, 2005, p. 113–146.

Jade (Nephrite and Jadeitite) and Serpentinite: Metasomatic Connections

G. E. HARLOW[1]

American Museum of Natural History (AMNH), Department of Earth and Planetary Sciences, 79th and Central Park West, New York, New York 10024-5192

AND S. S. SORENSEN

National Museum of Natural History (NMNH), Smithsonian Institution, Department of Mineral Sciences, 10th and Constitution Avenue, NW, P. O. Box 37012, NHB-119, Washington, District of Columbia 20013-7012

Abstract

The lapidary term "jade" refers to two very tough, virtually monomineralic rocks used for ornamental carvings or gems. Both have metasomatic origins that are intimately connected with their host serpentinite bodies and convergent-margin petrotectonics. Amphibole jade is nephrite, a tremolite-actinolite rock with a felted, microcrystalline habit; pyroxene jade is jadeite rock (jadeitite), which varies from micro- to macrocrystalline textures. Most nephrite occurs along fault contacts between serpentinite and mafic to felsic igneous rocks or metagraywacke in obduction settings. It forms by Ca- and Si-rich, aqueous fluid–mediated metasomatic replacement of serpentinite, typically antigorite, at greenschist-facies or lower P-T conditions. Other nephrite bodies reflect contact metasomatic replacement of dolomite by Si-rich aqueous fluids during felsic pluton emplacement.

Like most nephrite, jadeitite is hosted by antigorite-dominated serpentinite bodies. However, these serpentinites are associated with HP/LT metamorphic terranes, in which jadeitite occurs as isolated tabular bodies or tectonized blocks. Based on textural evidence, particularly clear from cathodoluminescence studies, nearly all jadeitite bodies appear to have formed originally as vein crystallization of an aqueous fluid, most readily interpreted as Na-Al-Si–rich fluid at HP/LT conditions in subduction/collisional settings. The host serpentinite influences jadeitite compositions by lowering fluid a_{SiO2} during serpentinization, and contributing Ca + Mg ± Cr to late-stage jadeitite-forming fluids. Thus, although both types of jade form in convergent-margin tectonic settings, jade has two distinct primary modes of origin: (1) by siliceous replacement of already serpentinized ultramafic rock at low-P, low- to moderate-T conditions following obduction (nephrite); or (2) by the interaction of serpentinizing peridotite and Na-Al-Si fluids at HP/LT conditions during active subduction/collision (jadeitite).

Introduction

THE TERM "JADE," as used in geology and gemology, refers to two extremely tough, essentially monomineralic rocks that are used for fashioning ornamental carvings and gems. Amphibole jade is nephrite, a tremolite-actinolite [$Ca_2(Mg,Fe)_5Si_8O_{22}(OH)_2$] rock with a felted, microcrystalline habit, and pyroxene jade is a jadeite [$NaAlSi_2O_6$] rock (jadeitite), which varies from micro- to macro-crystalline textures. Although their compositions and textures differ, both types of jade are typically associated with serpentinite, and both reflect aqueous fluid crystallization and metasomatic processes.

Robert G. Coleman pioneered the modern understanding of jadeite and nephrite petrogenesis with his petrologic studies of jadeitite at Clear Creek in the New Idria serpentinite body of California (Coleman, 1961), and of serpentinites and nephrites from the South Island of New Zealand (Coleman, 1966), as well as in his numerous papers that link serpentinites, serpentinization, and plate-boundary processes (e.g., Coleman, 1967, 1977, 1980). "Dr. Bob" has also made a significant impact on many geoscientists who study rocks and processes related to serpentinites and jade, and in particular these two authors. Consequently, we dedicate this review and synopsis of jade-serpentinite relationships to him in honor of his 80th birthday. In it, we hope to show not only that the two types of jade share some

[1]Corresponding author; email: gharlow@amnh.org

common petrogenetic characteristics, but that both are products of and record important Earth processes at convergent margins.

Nephrite Jade

Occurrences and setting

Nephrite is the more geologically common and generally less valuable variety of jade. It has also been more widely utilized than jadeitite through human history. Important deposits occur at the Polar, Kutcho, and Ogden Mountain properties in northern British Columbia, Canada (Leaming, 1978; Gabrielse, 1990); along the Yurungkash and Karakash (White Jade and Black Jade) Rivers, Kunlun Mountains, Xinjiang, China (see Webster, 1975; Tang et al., 1994; Tsien et al., 1996b); Chuncheon, Korea (Kim et al., 1986; Wen and Jing, 1993, 1996; Yui and Kwon, 2002); northeastern Taiwan (Tan et al., 1977; Wang, 1987); southwest of Lake Baikal in the East Sayan Mountains, Siberia, Russia (see Prokhor, 1991); and near Cowell, South Australia (Flint and Dubowski, 1990). Restricted, small, or exhausted deposits with either historical significance or some literature include the Westland (Muddy Creek, Otago, New Zealand; Cooper, 1995); the Livingstone, Nelson, Otago, and South Westland fields on South Island, New Zealand (Coleman, 1966; Beck, 1984, 1991); Jordanow (formerly Jordansmuhl), Poland (Kunz, 1906; Visser, 1946); in the Granite Mountains (Fremont Co.), Seminoe Mountains (Carbon Co.) and Laramie Mountains (Albany Co.), Wyoming (Sherer, 1972; Madson, 1978; Hausel, 1993); and along the Noatak and Kobuk rivers south of the Brooks Range in Alaska (Loney and Himmelberg, 1985). Archeologically significant deposits that demonstrate the use of nephrite as a tool or prestige material are also numerous, particularly in China and Europe. However, in this review we focus on deposits with adequate scientific description, which can aid in understanding the diversity of nephrite petrogenetic processes (Table 1, Fig. 1).

Mineralogy and varieties

Nephrite consists predominantly of tremolite-actinolite, with generally minor to trace constituents of diopside, grossularitic garnet, magnetite, chromite, graphite, apatite, rutile, pyrite, datolite, vesuvianite, prehnite, talc, the serpentine polymorphs, and titanite. Amphibole composition ranges from essentially pure tremolite ($Ca_2Mg_5Si_8O_{22}(OH)_2$), a pure white variety first described in China and now known in the lapidary trade as "mutton-fat jade," to intense green, variably sodic actinolite ($Ca_2(Mg,Fe^{2+})_5Si_8O_{22}(OH)_2$), to less common varieties that are nearly black in color, owing either to a substantial ferro-actinolite component, or oxide/graphite microinclusions (Fig. 2). In rare cases, nephrite displays an intense emerald-green color from Cr^{3+} substitution via a $NaCrCa_{-1}Mg_{-1}$ exchange in the amphibole, particularly some of that found in British Columbia. Ochre to bright orange staining from iron oxidation in the weathering rinds of alluvial/eluvial nephrite boulders is common. Bony white to light ochre–colored archaic artifacts, the so-called "tomb jades," are chalk-colored alteration assemblages produced by ammonia-triggered leaching due to interactions with a decaying human body within a sarcophagus or tomb environment (Gaines and Handy, 1975). Another variety of whitened nephrite, termed "chicken bone" jade (Fig. 2), is thought to reflect heating or "bleaching" of the finished object (Tsien et al., 1996a).

Nephrite is produced by contact and/or infiltration metasomatism in two very different settings: (1) dolomite replacement by silicic fluids associated with "granitic" plutonism; and (2) serpentinite replacement by Ca metasomatism at contacts with more silicic rock, such as plagiogranite, graywacke, argillite, or chert. The dolomite replacement nephrite deposits are apparently less abundant and less volumetric than the serpentinite replacement deposits, which raises an interesting historical observation.

The most nephrite-centric culture on Earth was that of China between Neolithic times and about 1800, when jadeitite from Burma became available to the Imperial Court and essentially transformed Chinese preferences (e.g., Keverne, 1991; Wen, 2001). Unlike other cultures that employed the properties of jade for "chopping and cutting" during the Neolithic, China probably had a "jade age" that paralleled the "bronze age" in Western cultures. China alone retained both a jade-valuing tradition and jade-working expertise and technology after they developed metal-working technology. This Chinese "jade culture" even managed to survive the Communist Cultural Revolution of the late 20th century. For example, in the Yangzhou, China jade factory, a small fraction of master carvers employ traditional methods of carving jade in the midst of highly mechanized, mass-market production (Ward, 2001). The jade used in China during the Neolithic

TABLE 1. Important Jade Occurrences

Site	References
Nephrite deposits of "granite" metasomatized dolomite type	
White Jade River, Khotan Mountains, Xinjiang, China	Tang et al., 1994; Tsien et al., 1996a; Wu et al., 2002
Black Jade River, Khotan Mountains, Xinjiang, China	Tang et al., 1994; Tsien et al., 1996a; Wu et al., 2002
Chuncheon, Korea	Kim et al., 1986; Noh et al., 1993; Wen and Jing, 1993, 1996; Yui and Kwon, 2002
Cowell, South Australia	Flint and Dubowski, 1990
Barguzin-Vitim Massif, Central Vitim Highland, East Sayan, Russia	Sekerin et al., 1997
Buromskyoe deposit, Central Vitim Highlands, East Sayan, Russia	Serekin and Serekina, 1986
Korolyevo field, Kansay ore field, Kuraminskiy Mountains, Uzbekistan	Protod-yakonova and Mansurov, 1973
Meiling jade deposit, southern Liyang, Jiangsu, China	Zhong, 1995
Kuandian and Xiyuan, Liaoning, China	Wen and Jin, 1993, 1996; Wang et al., 2002; Zhang, 2002a, 2002b
Wenchuan, Sichuan, China	Wen and Jin, 1993, 1996
Laiyang, Shandong, China	Rawson, 1995
Nephrite deposits of serpentinite metasomatism or similar	
East Sayan, Siberia, Russia	Kunz, 1906; Gurulev and Sagzhiyev, 1973; Suturin, 1988; Prokhor, 1991; Sekerin et al., 1998
South Island, New Zealand	Turner, 1935; Coleman, 1966; Beck, 1984 & 1991; Cooper, 1995
British Columbia	Leaming, 1978; Gabrielse, 1990
Granite Mountains, Wyoming	Sherer, 1972; Madson, 1978
Alaska	Loney and Himmelberg, 1985
Fengtian, Taiwan	Tan et al., 1978; Wang,. 1987; Yui et al., 1988, 1990
Tamworth, South Australia	Hockley et al., (1978)
Jadeite jade (jadeitite) Deposits	
Hpakan-Tawmaw tract, Kachin State, northern Myanmar (Burma)	Bauer, 1895; Noetling, 1896; Bleeck, 1907, 1908; Lacroix, 1930; Chhibber, 1934; Bender, 1983; Thin, 1985; Hughes et al., 2000; Shi et al., 2001, 2003
Nansibon, Chin State, northern Myanmar	Avé-Lallemant et al., 2000; Hughes et al., 2000
Central Motagua Valley, Guatemala	
North side–El Progreso and Zacapa	McBirney et al., 1967; Silva, 1967, 1970; Harlow, 1994, 1995
South side–Zacapa and Jalapa	Seitz et al., 2001; Harlow et al., 2003b, 2004.
Ketchpel River, Pay-Yer massif, Polar Urals, Russia	Morkovkina, 1960; Dobretsov and Ponomareva, 1965; Kovalenko and Sviridenko, 1981.
Yenisey River, Khakassia (Borus Mountains, West Sayan)	Dobretsov, 1963; Dobretsov and Tatarinov, 1983; Dobretsov, 1984
Itmurundy, near Lake Balkhash, Kazakhstan	Moskaleva, 1962; Dobretsov and Ponomareva, 1965; Kovalenko and Sviridenko, 1981; Ermolov and Kotelnikov, 1991
Omi and Kotaki Rivers, Itoigawa area, Niigata Prefecture, Japan	Iwao, 1953; Shidô, 1958; Chihara, 1971; Komatsu, 1987
Oosa-cho, Okayma Prefecture, Japan	Kobayashi et al., 1987
Oeyama ophiolite, Tottori Prefecture, Japan	Tsujimori and Itaya, 1999; Tsujimori, 2002
Clear Creek, New Idria serpentinite, San Benito Co., California	Coleman, 1961
Punta Rasciassa, the Monviso serpentinite, Western Alps, Italy	Compagnoni and Rolfo, 2003
Maraşatlar, 60 km south of Bursa, Western Anatolia, Turkey	Okay and Kelly, 1994; Okay, 1997, 2002 (appears to be a jadeite whiteschist rather than jadeitite)

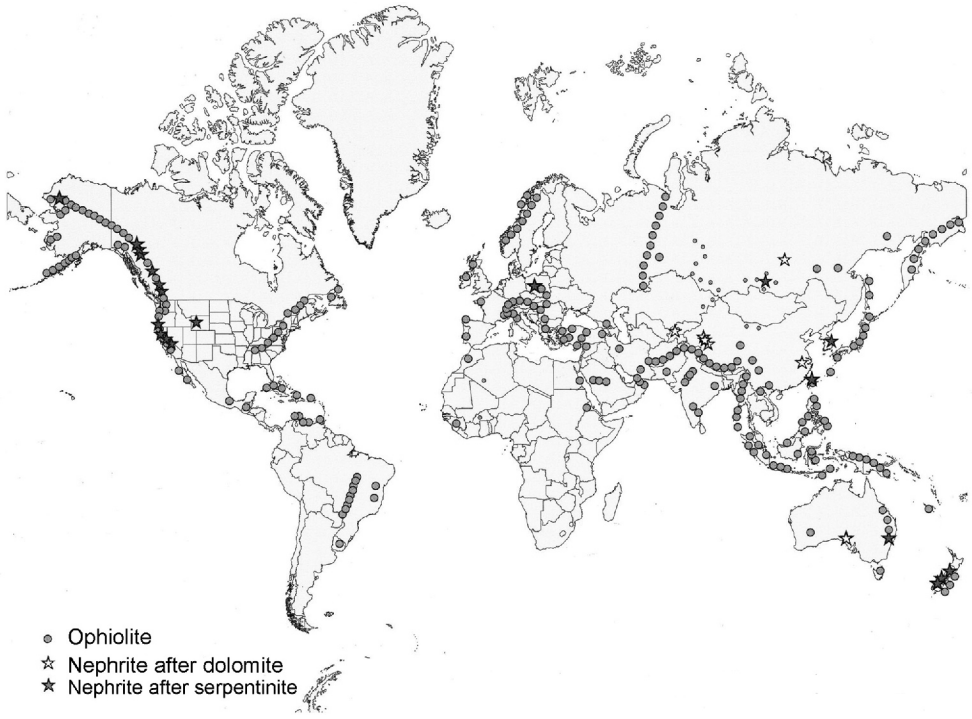

FIG. 1. World map showing the distribution of significant nephrite deposits and Phanerozoic ophiolite zones. Dolomite-hosted nephrite deposits are designated with a white-centered star and serpentinite-hosted with a dark-centered star.

and Bronze ages was obtained from regional deposits in dolomitic marbles (e.g., Douglas, 1996, 2003; Wen and Jing, 1996). Thus, the characteristic material of the Chinese jade culture was apparently obtained from the local but generally less common type of nephrite deposit. Now the Chinese cultural demand for nephrite is supplied in large part by serpentinite replacement deposits in British Columbia.

Nephrite by dolomite replacement

Examples of nephrite from this environment include a number of Chinese localities, namely: the Yurungkash (White Jade) and Karakash (Black Jade) rivers, Kunlun Mountains, Xinjiang, China (also called the Hetian source, Tang et al., 1994; Wu et al., 2002); the Xiaomeiling region of South Liyang, Jiangsu Province, China—a source for Neolithic Liangzhu culture (3400–2250 BCE; Zhong, 1995); Kuandian and Xiyuan in Liaoning (Wen and Jing, 1993, 1996; Wang et al., 2002; Zhang, 2002a, 2002b), Wenchuan in Sichuan (Wen and Jing, 1993, 1996), and Laiyang, Shandong (Rawson, 1995); as well as other noteworthy sources at Chuncheon, Korea (Kim et al., 1986; Noh et al., 1993; Wen and Jing, 1993, 1996; Yui and Kwon, 2002); Cowell, South Australia (Flint and Dubowski, 1990); the Korolyevo field, Kuraminskiy Mountains, Uzbekistan (Protod-yakonova and Mansurov, 1973); and the Barguzin-Vitim Massif, Central Vitim Highland (East of Lake Baikal), Siberia, Russia (Sekerin et al., 1997).

The model reaction for this paragenesis is typically presented as:

$$\underset{\text{dolomite}}{5Ca(Mg,Fe)(CO_3)_2} + 8SiO_2{}^{aq} + H_2O \rightarrow$$

$$\underset{\text{actinolite}}{Ca_2(Mg,Fe)_5Si_8O_{22}(OH)_2} + \underset{\text{calcite}}{3CaCO_3} + 7CO_2{}^{aq}. \quad (1)$$

However, this reaction models only the major-element components of the metasomatizing fluid. It does not explain the nearly monomineralic nature of dolomite-replaced nephrite, because a large amount of calcite—a phase virtually absent from observed

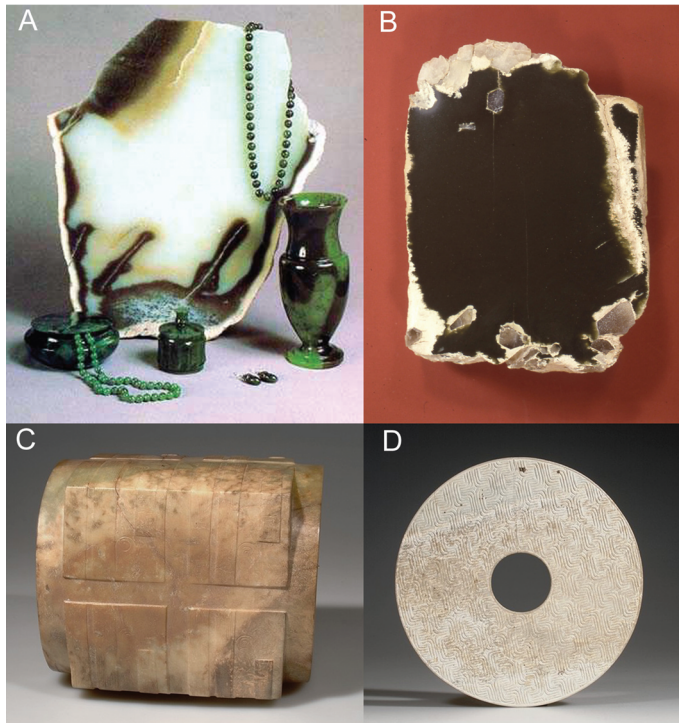

FIG. 2. Photographs of several varieties of nephrite: A. Mutton-fat (white) and Spinach (green with black oxide speckles) nephrites, Gorlikgol nephrite deposit, Gorlikgol River, Sayan Mountains, largest piece 50 cm high (from Knuzev, courtesy of Alexander Sekerin). B. "Black" jade, Granite Mountains, Lander County, Wyoming, 18 cm high (AMNH 21497, staff photo). C. Ts'ung, Liangzhu Culture, Tomb jade, 24.5 cm across (AMNH Anthro. 70.3/ 3562, China). D. Bi Disk, Early Western Han?, Chicken-bone jade, 27 cm across (AMNH Anthro. 70.3/ 3220).

nephrite—is produced by the reaction. Sekerin and Sekerina (1986) reported pockets, lenses, and stringers of nephrite interspersed with fine-grained calcite within dolomite in the Buromskyoe deposit, central Vitim Highlands, Russia. It is also possible that the reaction-product "calcite" is a component dissolved in the fluid at large fluid-to-rock ratios, and removed from the rock volume.

Although some nephrite occurs at contacts between an igneous dike or pluton and dolomite, it more commonly is disposed along faults and fissures that appear to have channeled post-magmatic fluids through dolomite (Sekerina, 1992). Also, nephritized carbonate xenoliths have been reported from the deposits of the Vitim Highlands (Sekerin and Sekerina, 1986). White nephrite from the Yurungkash deposit is an example of metasomatism of a dolomitized, cryptocrystalline, benthic, pure Precambrian limestone that was transformed to nephrite of both very small fiber size (typically 0.05 to 0.5 μm diameter; Wen and Jing, 1996) and high quality (Tsien et al., 1996b). Hydration and silicification of dolomite can yield green to black jade if the dolomite is ferruginous, as in the case at the Cowell field, South Australia (see below). Dark olive-green to black nephrite jade artifacts from China, which are attributed to a metasomatized dolomite origin due to their low Ni and Cr contents, are also rich in Fe and Mn (Douglas, 1996). This indicates that a mafic, rather than ultramafic, component existed either in the protolith of this jade, or the metasomatizing fluids (Douglas, 1996, 2003). The P-T conditions of formation for dolomite-derived nephrite are restricted by the high-T limit of the greenschist or amphibolite facies (<550 °C) and low to moderate pressures (100–200 MPa; e.g., Noh et al., 1993; Sekerin et al., 1997; although higher pressure, 200–400 MPa, is still consistent with facies and batholith emplacement).

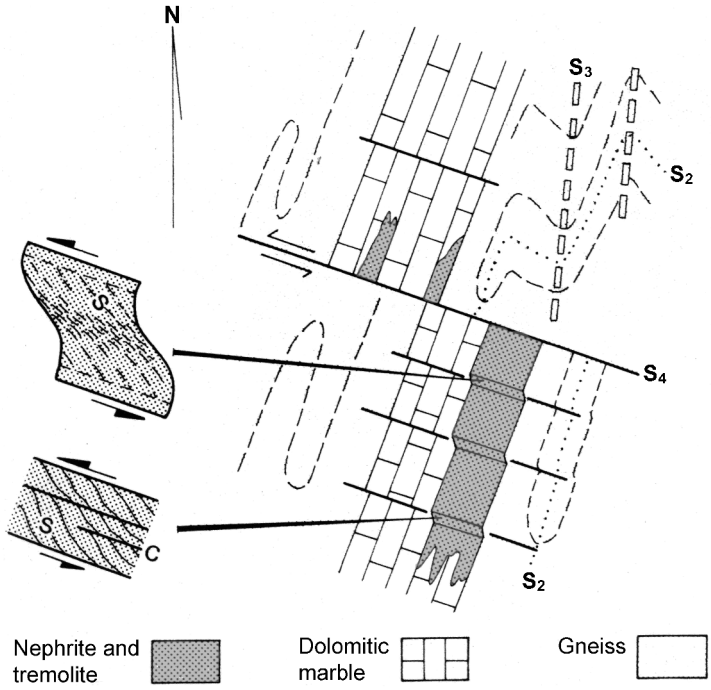

FIG. 3. Schematic geological plan of a typical Cowell nephrite body, showing the main structural elements and illustrating nephrite formation by SiO_2 metasomatism along S_4 fractures, correlated with dike emplacement in dolomitic marble; from Flint and Dubowski (1990, Fig. 2).

Two dolomite-replacement nephrite deposits have been described in sufficient detail to be reviewed: Cowell, South Australia and Chuncheon, Korea. The Cowell nephrite province occurs 25 km north of Cowell (~220 km north of Adelaide), South Australia and is volumetrically one of the largest jade deposits known (Flint and Dubowski, 1990). It is hosted by dolomitic marbles and banded calcsilicates of the Early to Middle Proterozoic Minbrie Gneiss complex. The nephrite forms elongated lens-shaped bodies, the origins of which are related to intrusion of quartz-pegmatite dikes. These deposits are attributed to silica metasomatism along fractures related to the dike emplacement (see Fig. 3) that then followed other structures to yield both (1) massive nephrite as a replacement of undeformed marble and (2) schistose (lower quality) nephrite in shear zones. The nephrite is unusually iron rich (1.26 to 7.1 wt% FeO in actinolite), which is attributed to the ferroan nature of the hosting Katunga Dolomite.

The Chuncheon, Korea deposit occurs at the contact of dolomitic marbles and amphibole schists of the Precambrian Yonduri gneiss complex in the central Gyeonggi block of the Korean Peninsula. The nephrite zone appears to replace dolomite near its upper contact with amphibole schist. It is bounded above by a thin zone of chlorite, and below by a calc-silicate zone that consists of grossular-diopside-tremolite ± chondrodite-quartz-calcite (Fig. 4). Phase equilibria indicate nephrite formed between 330 to 430°C at an assumed 200 MPa (Noh et al., 1993), consistent with regional metamorphism. Nephrite formation is attributed to metasomatic fluid circulation, presumably from fluids that emanated from the nearby post-tectonic, Late Triassic Chuncheon granite. Isotopic studies by Yui and Kwon (2002) yielded homogeneous, depleted values of $\delta^{18}O$ (–9.9 to –7.9‰) and δD (–118 to –105‰) in tremolite (nephrite), which were interpreted to track a fluid of meteoric origin that circulated hydrothermally and affected the rock at a high fluid/rock ratio. According to the authors, this interpretation is consistent with an H_2O-rich fluid (X_{CO2} <0.01–0.1) having equilibrated with both carbonate and silicate minerals.

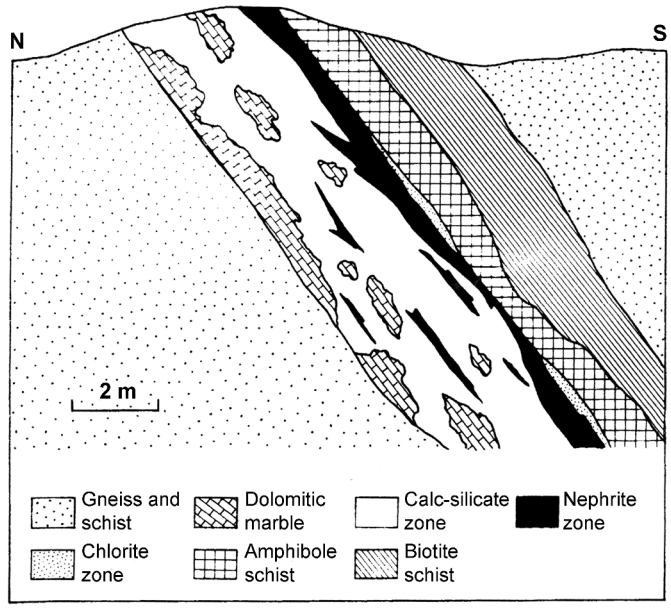

FIG. 4. Schematic cross section of nephrite deposit at Chuncheon showing the zones formed between dolomitic marble and amphibole schist; from Yui and Kwon (2002, Fig. 2) after Noh et al. (1993).

Yui and Kwon (2002) also presented isotopic data for the Xinjiang (Hetian) nephrite, which displays similarly low δD but slightly heavier $\delta^{18}O$ (0.5 to 2.3‰) values. They argue that these data, particularly the heavier $\delta^{18}O$ values, reflect meteoric water metasomatism at lower fluid/rock ratios than the Chuncheon deposit.

Nephrite associated with serpentinite

Nephrite is commonly associated with serpentinite (or serpentinite mélange) units within ophiolite belts. Ophiolites are fragments of on-land oceanic, back-arc, and arc lithosphere that either suture continental lithospheric blocks that have collided, represent arc-continent collisions, or appear to be isolated bodies that have ramped up upon (obducted onto) continental margins (e.g., Coleman, 1977; see Fig. 1). Ophiolites are generally features of Proterozoic and younger mountain belts, such as those of the Alpine-Himalayan system, the circum-Pacific and Caribbean margins, and the Cordillera of the western United States and Canada. Although ophiolite-hosted nephrite occurrences share a broad general geologic context, a variety of assemblages are reported, which suggests that there is no single mechanism of petrogenesis. Nevertheless, most models for nephrite formation propose metasomatic interaction of serpentinite or serpentinizing peridotite with more silicic rocks, such as plagiogranite (trondhjemite or albitite?), graywacke, shale, phyllite, or chert. This interaction is thought to be promoted by Ca-rich hydrous fluid-flow along contacts, structural boundaries, fractures, and/or faults, to produce pods or layers of nephrite between the two contrasting rock types (see below). Coleman (1966, 1967) pointed out that the contacts at which serpentinite-hosted nephrites (and other boundary reaction products) occur do not record high-temperature metamorphism and thus either postdate "cold" tectonic juxtaposition or overprint preexisting high-T contact assemblages.

In the serpentinite-hosted association, systematic metasomatic zoning sequences are common along nephrite-bearing contacts that appear to be intact (Table 2). The mineral assemblages of these sequences vary greatly, although compositional zoning with respect to SiO_2, MgO, and CaO (and perhaps Al_2O_3) is a common theme (see below). Many contacts between nephrite and serpentinite show slickensides, which indicate they are tectonized surfaces. Reaction histories along such contacts may be only partly preserved.

A review of some key serpentinite-related nephrite deposits illustrates both commonalties and

TABLE 2. Systematic Zoning Sequences Producing Nephrite

Location	Massive serpentinite		Metasomatic zone			Silicic rock
Taiwan:						
Yui et al. (1988)	Antigorite		Nephrite	Diopsidite	Epidotite	Muscovite-quartz schists
Tamworth, Australia:						
Hockley et al. (1978)		Schistose Serpentinite	Talc	Nephrite	± Diopside ±	Quartz phyllite
East Sayan, Siberia:						
Prokhor (1991)	Serpentinite matrix mélange	Antigorite	Nephrite	Rodingite		Plagiogranites and quartz diorites
Karpov et al. (1989)		Talc	Nephrite	Chloritite	Rodingite	
Red Mt. Creek, CA						
this work	Serpentinite	Diopsidite	Nephrite	Diopsidite	Graywacke	

outstanding petrogenetic problems. On the South Island of New Zealand, nephrite is found along the Alpine fault in the Taramakau-Arahua and Lake Wakatipu regions (Beck, 1984) primarily in glacial and fluvial deposits. Outcrops are rare (e.g., on Jade and Olderog creeks in the Arahua River drainage; Beck, 1984) with semi-nephrite (either massive amphibole, which lacks the felted cohesive texture, or nephritic amphibole enclosing coarser crystals) more common in outcrop than true nephrite. Restrictions on exportation make this area of historical and archeological interest, rather than a commercial deposit. Coleman (1966) described examples of semi-nephrite that occur at the altered edge of tectonic inclusions of argillite, where a quartz-albite meta-argillite block is progressively replaced toward a metasomatized rim by actinolite-tremolite and diopside, with irregular lenses of semi-nephrite (along with segregations of prehnite and diopside) at the serpentinite contact (Fig. 5). The contact between the argillite blocks and serpentinite, where the semi-nephrite occurs, has mylonitic to cataclastic texture. It is not clear whether the nephrite/semi-nephrite replaces argillite, serpentinite, or both. However, chromium coloration has been reported in New Zealand nephrites (Beck, 1984), so serpentinite replacement is likely in some instances.

Pressures and temperatures of formation, as well as a possible nephrite-producing reaction, can be loosely constrained for the New Zealand nephrite occurrences. Coleman (1966) reported that serpentinite adjacent to these deposits is a lizardite-chrysotile mixture, which suggests low-T conditions of serpentinization. In addition, aragonite occurs in limestone blocks and lawsonite in the Maita sediments within the serpentinite mélange, which could indicate that nephrite rinds also formed at relatively HP/LT conditions.

Cooper (1995) documented an occurrence of semi-nephrite and tremolite-fuchsite-chlorite schist around a metasomatized gabbro/peridotite block in the Haast quartzofeldspathic schist at Muddy Creek off the Haast River, New Zealand (Fig. 6). This author concluded that shearing of the blackwall-like tremolite rock produced a cataclastic "nephrite," whereas secondary crystallization of fine-grained tremolite produced a true nephritic texture encapsulating the other minerals in these rocks. Cooper (1976, 1995) also reported a pumpellyite-tremolite-chlorite assemblage in the gabbro-peridotite core of a block, which implies a temperature <300°C. The presence of talc and steatite implies that CO_2 concentrations in the fluid were sufficient to enable the reaction:

$$\underset{\text{Serpentine}}{2Mg_3Si_2O_5(OH)_4} + 3CO_2 \rightarrow$$

$$3MgCO_3 + 3H_2O + \underset{\text{Talc}}{Mg_3Si_4O_{10}(OH)_2}. \quad (2)$$
$$\text{Magnesite}$$

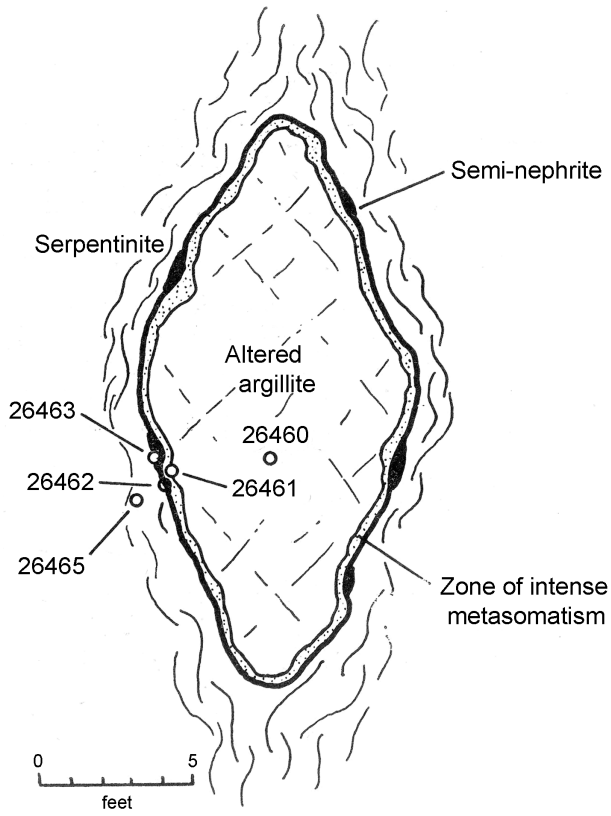

FIG. 5. Schematic diagram of tectonic inclusion of argillite at Dun Mountain, South Island, New Zealand, showing metasomatism and formation of semi-nephrite at boundary with serpentinite. Figure from Coleman (1966, Fig. 7).

This reaction and the involvement of CO_2 appear to be important in nephrite occurrences in which talc/steatite is part of the blackwall zoning assemblage (Cooper, 1995). However, the paucity of magnesite, which is only very rarely reported with nephrite sequences, renders the reaction somewhat problematic, although carbonate solubility must be considered.

A major commercial nephrite belt extends from the U.S. border through central British Columbia and into the Yukon. Nephrite deposits decorate ophiolites that are preserved in a Permo-Triassic suture zone of western North America. Variations in zoning and mineralogy occur, but the examples presented here are fairly representative of this "Cordilleran nephrite terrain" (see Leaming, 1978). At the Schulaps ultramafic massif, tectonic blocks of chert, argillite, and greenstone display metasomatized contacts with adjacent tectonized serpentinite, which is locally replaced by nephrite and talc-bearing nephrite. At Brett Creek, tectonic inclusions of chert within serpentinite are sequentially surrounded by zones of "white-rock" (a hydrous calc-silicate assemblage interpreted by some to be rodingite; see below), of nephrite, and of talc along serpentinite contacts. Chromite (picotite) in nephrite was interpreted by Leaming (1978) to be evidence of the metasomatic transformation of serpentinite to nephrite. Similar relationships exist at Cassiar, where Gabrielse (1990) interpreted "white rock" to be rodingitized diabase, ruptured and dislocated along tectonic boundaries. At Cassiar, the surrounding serpentinite is antigorite (Leaming, 1978; O'Hanley, 1996), but again, nephrite has replaced serpentinite by metasomatism along its contacts with more silicic rocks.

A few nephrite deposits show different features than the two deposit types above. The small nephrite

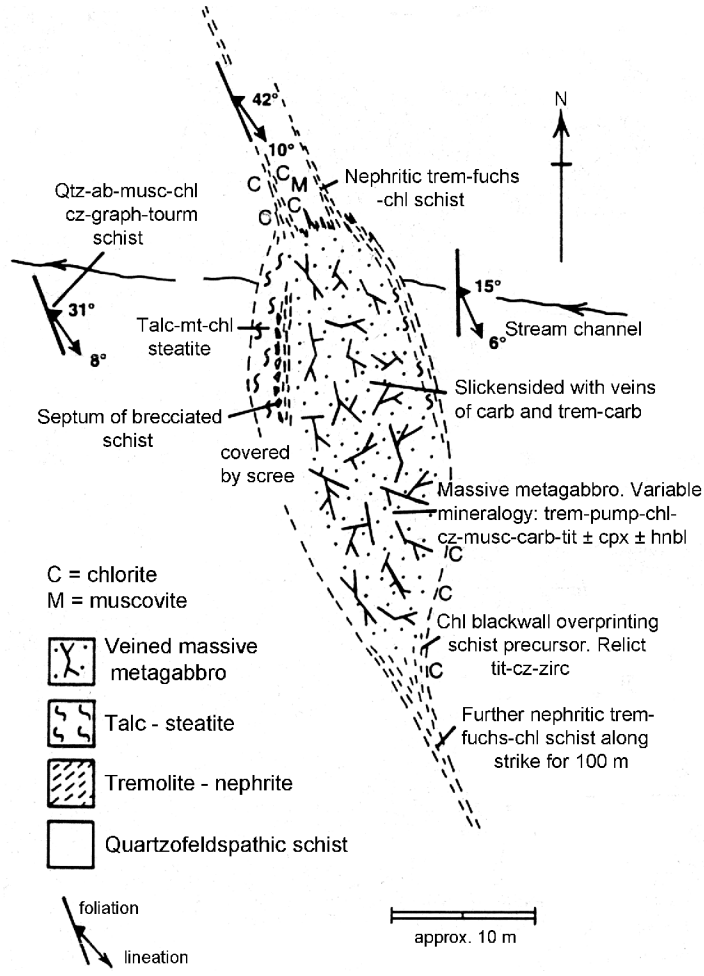

FIG. 6. Schematic diagram of the Muddy Creek, New Zealand, metagabbro pod showing distribution of nephritic schist at sheared boundaries with the body. From Cooper (1995, Fig. 2).

deposits in the Granite, Seminoe, and Laramie mountain ranges of Wyoming are interpreted to be metasomatic replacements of mafic igneous rock that had been previously metamorphosed to the amphibolite facies (Sherer, 1972; Madson, 1978). The Sage Creek (Wyoming) nephrite protolith is thought to have been amphibolite xenoliths in a quartz diorite dike derived from the adjacent Precambrian granodiorite batholiths (Sherer, 1972). Hausel (1993) argued that the Seminoe Mountain nephrite deposits were originally metakomatiites (tremolite-talc-chlorite-serpentine schists) that were nephritized by fluids that formed crosscutting quartz veins.

Conditions of nephrite formation in association with serpentinite

The P-T conditions of formation for nephrite associated with serpentinite are inferred to be of the greenschist facies, based on the actinolite ± chlorite assemblage of the nephrite itself, and the presence of lizardite/chrysotile serpentinite host rocks in numerous deposits. Taken together, these assemblages imply metamorphic/metasomatic temperatures of ~300–350°C to perhaps ~200–100°C. Closer constraints are based upon oxygen isotope fractionations and P-T estimates for contact metamorphism of ultramafic bodies by silicic plutons.

For example, Yui et al. (1988) calculated temperatures of 320 to 420°C, based on the oxygen isotope fractionation between nephrite (tremolite) and serpentine (antigorite) from the Fengtian nephrite deposits, Taiwan. The lack of nephrite and presence of coarse tremolite along a reaction zone between quartz diorite and the Trinity peridotite in northern California was interpreted by Peacock (1987) to reflect, on the one hand, a higher T than for nephrite based on the sense that temperature enhances growth of larger crystals and, on the other, T = ~400 to 425°C, the limiting temperature for tremolite in the assemblage. The very low T estimate is based primarily on the presence of pumpellyite in the Muddy Creek, New Zealand semi-nephrite (Cooper, 1995), and potentially anchizone assemblages of some graywacke-nephrite interfaces seen by GEH at the Red Mountain Creek deposit in California. Nephrite formed at serpentinite contacts is interpreted to reflect P ≤ 200 to 500 MPa (Karpov et al., 1989; Prokhor, 1991) based on mineral assemblages for a few deposits. In contrast, the occurrence of aragonite and lawsonite in tectonic blocks from serpentinites that host nephrite in New Zealand (Coleman, 1966) indicate that serpentinite probably experienced higher pressures, perhaps ~600 to 800 MPa, but it is possible that the nephritized serpentinite contact postdates the metamorphic phase assemblage. It is not clear whether nephrite can form at higher pressures; if it does, it is rare.

Suturin (1988) examined the nature of a fluid that could nephritize microantigorite, with attention to Coleman's (1980) hypothesis that such a fluid evolves from serpentinization. Suturin used thermodynamic modeling for chemical components and minerals, applying Korzhinskiy's interpretation of the interaction of acids and bases in solution that predicts that solids that are strong bases will be displaced by weaker ones during metasomatism. Suturin argued that the model of Coleman (1980) predicts that Ca-rich, oxidized fluids arise from clinopyroxene breakdown during the serpentinization of peridotite. However, his calculations and the presence of awaruite ($Ni_{2-3}Fe$) in antigorite serpentinite indicate that nephrite-forming solutions are strongly reducing and highly alkaline, but of relatively low Ca-concentration ($6–9 \times 10^{-4}$ molar at 350–400°C for nephritizing solution versus $2–4 \times 10^{-2}$ molar at 150–390°C for the serpentinizing solution). Therefore, the Mg-rich substrate (serpentinite or dolomite), which is a stronger base than Ca-rich nephrite, leads to nephritization. Suturin (1988) also argued that temperature controls the assemblage produced by the metasomatism; talc is stable from 370 to 400°C, and tremolite forms at 380°C and becomes dominant above 390°C.

Several models for nephrite-producing metasomatism at serpentinite–silicic-rock contacts are extant. Karpov et al. (1989) contrasted "simple water-rock metasomatism" with irreversible reactions produced by contact-infiltration metasomatism to evaluate nephrite formation. These authors examined an antigorite serpentinite–plagiogranite contact to determine the genesis of the alteration zones in a vein from the Ulankhodinskoye nephrite deposit, East Sayan. The thermodynamic models, which were calculated both at constant T of 375°C and over a gradient from 300 to 400 °C at 200 MPa, were constructed to determine how fluid-mediated metasomatism might occur within plagiogranite and antigorite, as well as along the boundary between them. In the first scenario, "simple water-rock interactions" were modeled as a fluid in equilibrium with serpentinite moving from the serpentinite into plagiogranite via veins (with possible along-boundary flow), and vice versa. Each produced a vein with layered reaction zones in the infiltrated rock. The reaction zones were disposed in opposite sequences in the two host rocks. Although the models reproduced zoning profiles seen in the deposit—bands of rodingite, steatite, chlorite-talc rock, etc.—they did not yield nephrite (see Fig. 7A). In these cases, Karpov et al. (1989) were forced to appeal to an external source for nephrite-forming components that would enter the host rocks from a "hypothetical source"; this external fluid was "ready" to form nephrite, a concept previously invoked by Suturin and Zamaletidinov (1984).

The concept of a "ready" or "ripe" nephrite-producing fluid has been a topic of controversy for many years. Coleman (1966, 1967, 1977) noted that aqueous fluids flowing through bodies of serpentinizing ultramafic rock should become saturated in Ca^{2+} as a result of clinopyroxene breakdown during serpentinization. However, if nephrite forms after serpentinization is largely complete, Ca-saturated fluids are unlikely to be serpentinite-sourced. Alternatively, a Ca-rich fluid may evolve by a chromatographic or similar process that saturates Ca-amphibole component in a multicomponent fluid at various P-T conditions (e.g., Brady, 1977; Lictner et al., 1986; Sedqui and Guy, 2001). If the nephrite-forming process occurs during active serpentinization, large amounts of aqueous fluid would be

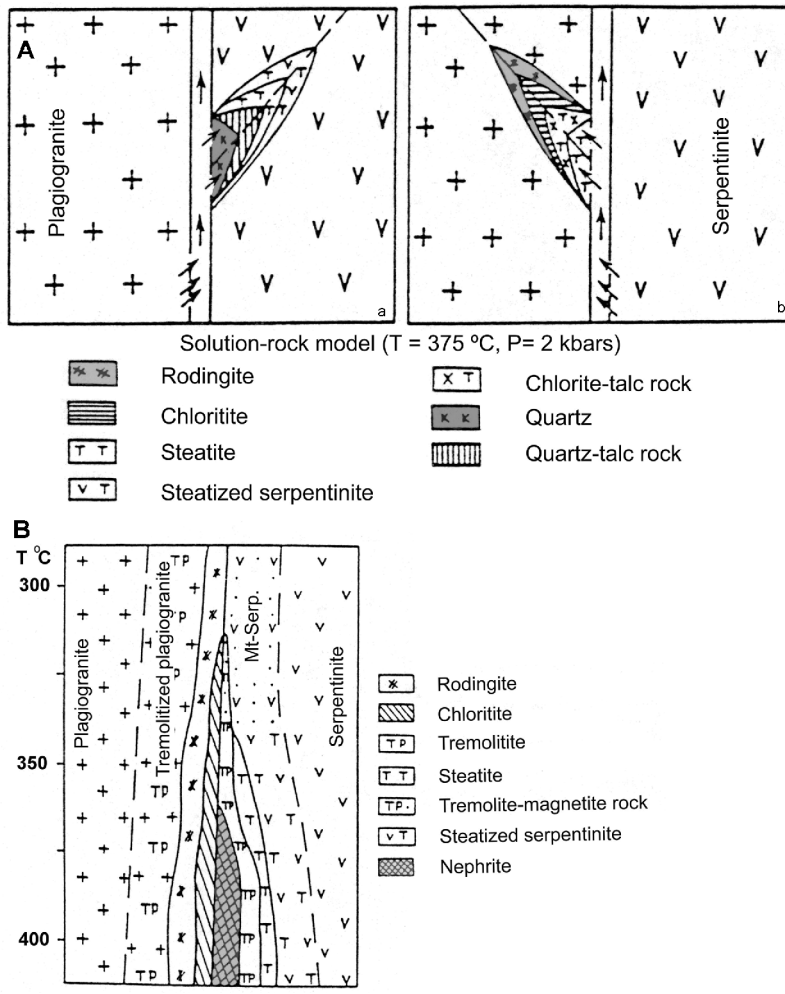

FIG. 7. A. Reaction with serpentinite of a solution that is in equilibrium with plagiogranite (a = after Karpov et al. (1989, Fig. 1), solution-rock model [T = 375ºC, P = 2000 bars]; b = reaction of serpentinite solution with plagiogranite). B. Overall scheme of metasomatic zoning derived by irreversible reaction modeling; after Karpov et al. (1989, Fig. 3).

consumed by the hydration of peridotite, which could potentially concentrate a variety of solutes in small amounts of residual fluid. A similar idea has been advanced to explain rodingite, a white, pink, or brown metasomatic alteration product of basalt and gabbro dikes and mafic tectonic blocks. Rodingite typically consists of a variable mixture of diopside, hydrogrossular (hibschite), clinozoisite, vesuvianite (idocrase), and prehnite (Coleman, 1967; O'Hanley, 1996; El-Shazly and Al-Belushi, 2004). Rodingite results from Ca enrichment and desilicification of the mafic protolith, linked to fluid-rock reaction between basalt and peridotite during serpentinization. Consonant with Coleman (1967), the Ca in rodingitizing fluids is probably derived from serpentinization. However, unlike rodingititization, nephritization requires both Ca and Si enrichment of a serpentinite/ultramafic protolith (Coleman, 1967; O'Hanley, 1996).

Karpov et al. (1989) also modeled contact-infiltration metasomatism with plagiogranite and serpentinite, using the same fluids and fluid flow directions, but with a reaction layer of fluid between the plagiogranite and serpentinite. The fluid both transports chemical species and promotes diffusive infiltration into the rocks. In the case of a plagio-

granite-sourced fluid, nephrite was not produced but the model predicted serpentinite replacement by diopsidite, which is found in some parts of the Ulankhoniskoye deposit. However, if the solution was initially in equilibrium with serpentinite, a zoning profile along the rock contact was predicted that mimics that of the vein that was being modeled (Fig. 7B). This preferred model requires both fluid infiltration and stepwise irreversible reactions (as opposed to equilibrium crystallization) that replace some initial phases at the contacts, such as corundum by chlorite. Nephrite is produced both in the channel between the plagiogranite and serpentinite and by corrosion of the boundary serpentinite. This model also obviates the need for the external "ready" fluid.

Prokhor (1991) visualized nephrite formation in East Sayan as a conjugate process to rodingite formation, with the crucial difference being the opposite directions of migration of silica in the two processes (i.e., out of the replaced rock in rodingite, into the replaced rock in nephrite). He suggested that both processes could be contemporaneous. O'Hanley (1996) argued strongly that to form nephrite, in contrast to rodingite, Ca must enter from outside the serpentinite after both serpentinization and rodingite formation are essentially complete. He based this conclusion on the sense of silica flux and textural criteria, such as apparent pseudomorphs of serpentinite by nephrite. Further modeling is needed to resolve the disagreements and explain diverse, serpentine-associated nephrite occurrences.

Nephrite texture

The primary microstructural feature of nephrite is a micro- to crypto-crystalline texture that consists of a fibrous-mat intergrowth of tremolite-actinolite crystals with extreme length/width ratios; some workers (e.g., Dorling and Zussman, 1985; Germine and Puffer, 1989; O'Hanley, 1996) have described nephrite as resembling a microcrystalline variety of felted asbestos (Fig. 8). Three origins have been suggested for this texture. Pseudomorphism after antigorite-serpentinite has been proposed for the nephrite from the East Sayan, Russia (Suturin, 1988; Prokhor, 1991) and the Cassiar deposit, British Columbia (Leaming, 1978; O'Hanley, 1996). The evidence for this is: (1) the strong resemblance between nephrite mesostructure and that of antigorite serpentinites and schists (Fig. 8); (2) the presence of magnetite/chromite grains in nephrite; and (3) the presence of antigorite adjacent to nephrite bodies in these deposits. In general, fibrous minerals grow either in an aqueous environment or during retrograde metamorphism in the presence of a fluid (e.g., Veblen and Wyllie, 1993), typically at relatively low T conditions. Thus, pseudomorphism after antigorite fits one of the modes of fiber growth; growth of nephrite in a fluid-filled open space would be another. Exactly how fiber-mat crystallization, characteristic of nephrite, differs from cross-fiber growth in a vein (as in the asbestiform habit: Veblen and Wiley, 1993; Zoltai, 1981) is not explained, but presumably mat growth does not involve crystal nucleation on a fracture or cavity wall and perpendicular growth into open space. Perhaps fewer discrete nephrite nuclei in the fluid yield radiating or plumose growths that create interlocking fibers. Other authors attribute some nephrite textures to shearing and internal recrystallization of blackwall-like mineralization, or the infiltration of tremolite-producing fluids during recrystallization (e.g., Turner, 1935; Cooper, 1995). From transmission electron micrographic (TEM) images of Wyoming nephrite, Dorling and Zussman (1985) intepreted rounded boundaries of submicron-wide actinolite fibers sharing a common *c*-axis orientation as the result of recrystallization after shear motion. In both such scenarios, the degree of secondary recrystallization determines whether the product is semi-nephrite ("cataclastic nephrite") or "true" nephrite.

An unusual variant of nephrite shows botryoidal textures, as exemplified at Red Mountain Creek, Trinity Co., in the Coast Range tectonic belt of California. R. Coleman, F. Wicks, and G. Harlow investigated this locality in 1996. The nephrite occurs along a fault that juxtaposes serpentinite (sheared, chrysotile + lizardite veins and antigorite cores) against tectonic inclusions of a sedimentary unit that varies between graywacke and black shale. Nephrite forms layers of small botryoidal nodules in the graywacke, and diopsidite fills the contact zone between graywacke and serpentinite. Outcrop, hand-sample, and polished-section textures suggest fluid flow occurred along fault contacts within serpentinite and between serpentinite and inclusions. Fluid also infiltrated the permeable graywacke block along the contact zone, reacted with the black graywacke/shale matrix, and created 3 to 30 mm diameter whitish "cumulus cloud"–like structures of nephrite (Fig. 9). Graywacke near the contacts is replaced either by nephrite or an aggregate of microcrystalline diopside ± pumpellyite that retains the

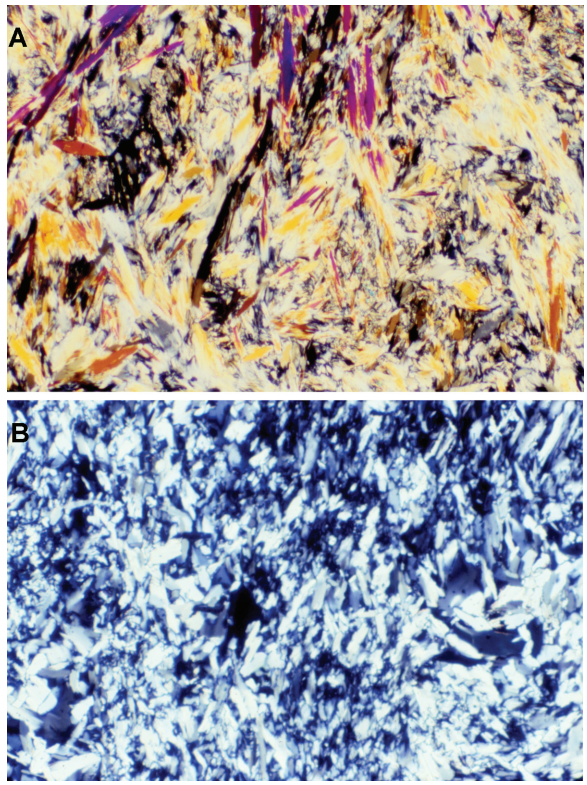

FIG. 8. Photomicrographs with crossed polars of (A) nephrite from Onot River, East Sayan (USNM-8459), a presumed metasomatized serpentinite, and (B) antigorite schist, Estancia de La Virgen, Zacapa, Guatemala (AMNH MVJ87-6-2). Both images are 2.1 mm across.

(black) color of the graywacke/shale. The diopsidite fills the vein system within the graywacke and infiltrates the serpentinite along fractures, in a manner similar to aspects of the model of Karpov et al. (1989). Apparently, diopsidite formed subsequent to nephrite formation.

A basic unanswered question raised by field observations worldwide is whether serpentinite, inclusions/country rocks, or the contact between them constitutes the nephrite protolith. O'Hanley (1996) argued strongly that during nephritization (as contrasted with rodingitization) Ca enters serpentinite after serpentinization is essentially complete. Karpov et al. (1989), and to some extent Suturin (1988), concluded that either the elusive "ready" fluid or antigorite-forming fluid metasomatizes serpentinite at the boundary with plagiogranite, in open fractures, and in and adjacent to the serpentinite. In contrast, the nearly ubiquitous occurrence of relict chromite in nephrite and the pseudomorphic textures support serpentinite replacement (e.g., Cooper, 1976; Leaming, 1978; Sekerin et al., 1997). The botryoidal nephrite from Red Mountain Creek and perhaps the semi-nephrite from Dun Mountain, New Zealand (Coleman, 1966) might be examples in which "ready" fluid, rich in Ca (and Mg), exits serpentinite to nephritize adjacent, Si-richer rock.

In general, nephrite crystallization sequences do not articulate well with the metamorphic histories of their ultramafic host rocks. For example, many nephrite bodies are hosted by serpentinites that consist predominantly of lizardite and chrysotile, yet nephrite textures suggest replacement of antigorite. Prokhor (1991) described partially nephritized antigorite aureoles around tectonic blocks of plagiogranite and quartz diorites in the East Sayan deposits. In Taiwan (Tan et al., 1977; Yui et al, 1988) and British Columbia (Leaming, 1978; O'Hanley, 1996), antigorite is found adjacent to nephrite. Perhaps local high a_{Al2O3} may explain

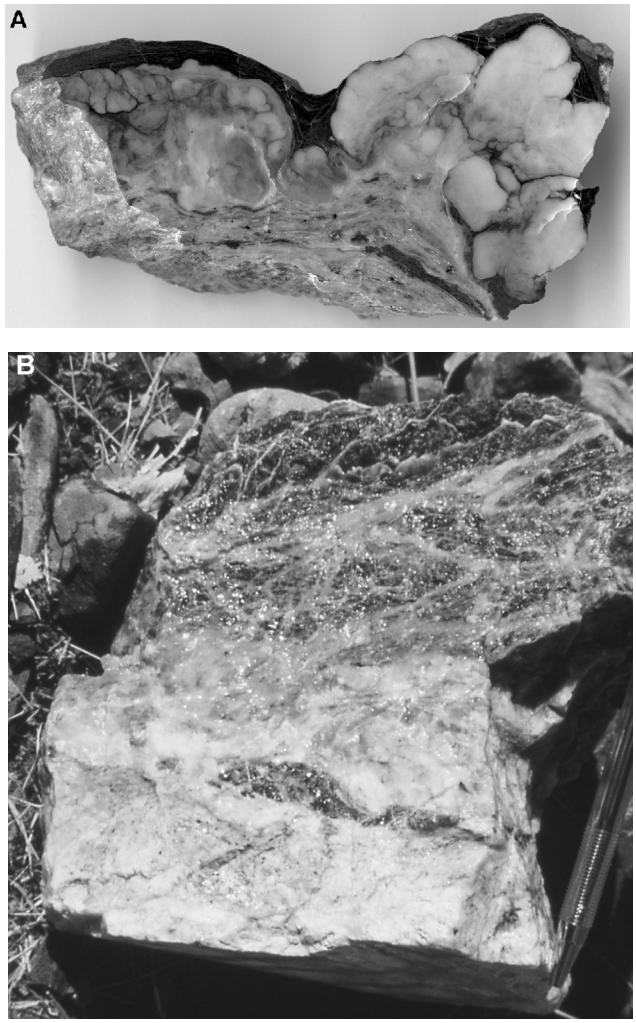

FIG. 9. Images of rocks showing textures of faulted contacts between serpentinite and graywacke and infiltration mineralization at Red Mountain Creek deposit, Trinity Co., California. A. A polished section of carbonaceous "graywacke" (black area at top) with penetrating botryoidal nephrite (whitish cloud-like body) and diopsidite-filled vein at the serpentinite contact (lamellar structure at bottom); the sample is 8 cm across. B. Fault bound (slickensides on base) block of diopsidite-serpentinite boundary (20 cm across): fault contact/fluid channel of diopsidite vein infilling (horizontal at bottom), a small fragment of diopsidite-replaced black graywacke, and diopsidite-replaced serpentinite (above) giving way to highly micro-veined (diopside) serpentinite (antigorite in core regions) away (above) from the channel.

antigorite aureoles around nephrite masses, because some studies suggest this polymorph is stabilized relative to lizardite and chrysotile by addition of Al_2O_3 (e.g., Evans et al., 1976; Bromiley and Pawley, 2003). If Al metasomatism precedes nephritization, early formed antigorite might in part be replaced by nephrite, to yielding a "pseudomorph-after-antigorite" texture. Alternatively, nephrite-forming contact metasomatism may occur at a range of P-T conditions, under which either antigorite or lizardite ± chrysotile are the stable serpentinite mineralogy.

A third basic, yet unanswered, question is whether there is a petrogenetic relationship between nephrite and rodingite. Prokhor (1991) presented evidence for the inverse coupling of Ca and Si migration, to form "conjugate" nephrite and rodingite in incompletely serpentinized ultramafic rock. In contrast, Coleman (1966, 1967) pointed out a lack of consistent correspondence between rodingite and nephrite occurrences in serpentinite-hosted metasomatic terranes. This could have several explanations. First, many rodingite and nephrite bodies show tectonized contacts with serpentinite, which makes it possible that parts of the metasomatic system could be displaced (e.g., New Zealand; Cooper, 1995). Variations of P-T conditions could destabilize characteristic rodingite minerals such as prehnite or vesuvianite, and the degree of coupled metasomatic exchange might produce different assemblages. The latter factor could be subtle, because the range of protoliths that produce rodingite versus nephrite is very similar (Coleman, 1966, 1967). Comparative isotopic and trace-element studies on paired nephrite-rodingite versus, for-example, nephrite-diopsidite should resolve whether the pairing is a conjugate versus a multistage process. Such isotopic data ($\delta^{18}O$ and δD) are available for the Fengtien nephrite deposit, in which nephrite appears to coexist with both diopsidite and epidote-fels (Yui et al, 1988; all these rocks are termed rodingite by the authors). These authors concluded that nephrite and diopsidite show evidence for having formed in isotopic equilibrium at 320 to 420°C, whereas the epidotite (clinozoisite) does not. Finally, it is likely that metasomatite pairing only occurs under specific ranges of conditions where the fluid-transported components yield assemblage saturations for rodingite and nephrite for a particular stage of serpentinization and silicic block composition.

Jadeite Jade

Overview and setting

Jadeitite, a rock consisting primarily of jadeite grains, is slightly harder than nephrite and nearly as tough (Kunz, 1906; Leaming, 1978). It has been used as a cultural mineral for roughly 7000 years (e.g., circa 4500 BCE by the Joman people, Japan; Keverne, 1991). Translucent jadeitite is the "precious" jade used in fine jewelry. Jadeitite is much rarer than nephrite: only ~12 occurrences have been described worldwide (Table 1; Fig. 10). The largest and most important deposit is the Hpakan-Tawmaw tract, Kachin State, northern Myanmar (Burma), and in conglomerates and alluvial deposits derived from that source (Chhibber, 1934; Bender, 1983; Goffe et al. 2000; Hughes et al., 2000). Related sedimentary rock units that contain jadeitite detritus are also mined at Nansibon, Chin State (about 60 km west of Hpakan; Hughes et al., 2000; Avé Lallemant et al., 2000) and conglomeratic units from the Monhyn (Thin, 1985) to the Indaw-Tigyaing areas (United Nations, 1979), ~100 to 230 km south of Hpakan, along the Sagaing fault.

Another important source, the one for New World jade, is centered on the middle Motagua Valley, Guatemala (Harlow, 1994; Seitz et al., 2001). There, jadeitite is present in two HP/LT lithotectonic belts that reflect distinctly different Cretaceous tectonic events. These belts are now juxtaposed by the North American–Caribbean plate boundary (Harlow et al., 2003b, 2004). Less developed resources are the deposits along the Ketchpel River, Pay-Yer massif, Polar Urals (Morkovkina, 1960; Kovalenko and Sviridenko, 1981) and on the Kantegir and Yenisey rivers, ~100 km north of Abakan, Khakassia, Russia (= Borus Mountains, West Sayan; Dobretsov, 1963, 1984; Dobretsov and Tatarinov, 1983), as well as at Itmurundy, near Lake Balkhash, Kazakhstan (Dobretsov and Ponomareva, 1965; Ermolov and Kotelnikov, 1991). Jadeitite is also documented from along the Omi and Kotaki Rivers, Itoigawa area, Niigata Prefecture, Japan (Iwao, 1953; Chihara, 1971; Komatsu, 1987); Oosa-cho, Okayma Prefecture, southwestern Japan (Kobayashi et al., 1987); along Clear Creek in the New Idria serpentinite, San Benito Co., California (Coleman, 1961); and from Punta Rasciassa, the Monviso serpentinite, Western Alps, Italy (Compagnoni and Rolfo, 2003; R. Compagnoni, pers. commun., 2003).

Varieties

Jadeite jade is typically considered to be jadeitite if it contains at least 90 vol% pyroxene, and the average pyroxene has at least 90 mol% jadeite, although such definitions are not invariably useful or applicable. Jadeitite composed of end-member jadeite is white in hand sample. The highly valued "Imperial" emerald green color is due to Cr^{3+} (as $NaCrSi_2O_6$; kosmochlor); as little as Ko_{2-3} produces intense color (Ou Yang, 1984; Mével and Kiénast, 1986; Harlow and Olds, 1987). Leaf-green colors result from Fe^{2+} (>>Fe^{3+}), blue-green from the presence of both Fe^{2+} and Fe^{3+} at comparable (but low)

FIG. 10. World map showing the distribution of described jadeitite deposits and Phanerozoic blueschist areas.

concentrations, yellowish green from low Fe^{3+}(>Fe^{2+}), and mauve from Mn^{3+} (Ou Yang, 2001). Near-sapphire-blue colors in jadeitite from the Itoigawa area, Japan and near Jalapa, Guatemala are correlated with elevated Ti in grains and veins of omphacite ($TiO_2 \leq 6$ wt%). However, optical absorption spectra of these samples resemble those for riebeckite, which is colored by Fe^{2+}-Fe^{3+} intervalence charge transfer (Harlow et al., 2003a). Black jadeitite can result from micro-inclusions of graphite. Intermediate colors to those above can arise from mixing of the chromophores. The compositions of clinopyroxene in jadeitites range from Jd_{100} to omphacite (nominally $Jd_{50}[Di+Hd]_{50}$ but as low as $Jd_{40}[Di+Hd]_{60}$). Aegirine ($NaFe^{3+}Si_2O_6$) component ($Ac_{5\text{-}15}$) typically increases with omphacite content.

A review of the zoning patterns among lithologies in jadeitite occurrences illustrates their variability. In the Hpakan area, Myanmar (Burma), where the "Jade Tract" occurs, jadeitite is found as pebbles to large boulders in the alluvium and eluvium and in massive serpentinite conglomerates, as large pod-like bodies and as so-called dikes in serpentinite (Noetling, 1893, 1896; Bleeck, 1907, 1908; Chhibber, 1934; Thin, 1985; Hughes, et al., 2001; observations by GEH). At Tawmaw, Myanmar, one side of the main jadeitite "dike" (which we interpret to be a complex vein structure), which locally displays an albitite carapace, is in a fault contact with serpentinite and blackwall, whereas the other contact shows a more or less intact metasomatic zoning relationship with a sodic-amphibole ± jadeite gneiss (see Fig. 11). At Nant Maw Mine #109 near Hpakan (visited by GEH in 2002) a ~20 m long pod-like body, totally underground, is connected to a <1 m wide vein system that breaches the surface. In it, white-to-mauve coarse-grained jadeitite is bordered by a 0.5–2 m wide sheared, green, Cr-bearing jadeitite with a boundary layer, <1 m thick, of jadeite-amphibole rock that is cut by cm-sized veins and selvages of albitite. A layer of blackwall, up to 5 cm thick where exposed, separates the jadeite-amphibole rock (or albitite selvages) from tectonized antigorite serpentinite. The thin vein that connects to the pod shows portions of the larger-scale mineral zonation, and lacks the green jadeitite and amphibole.

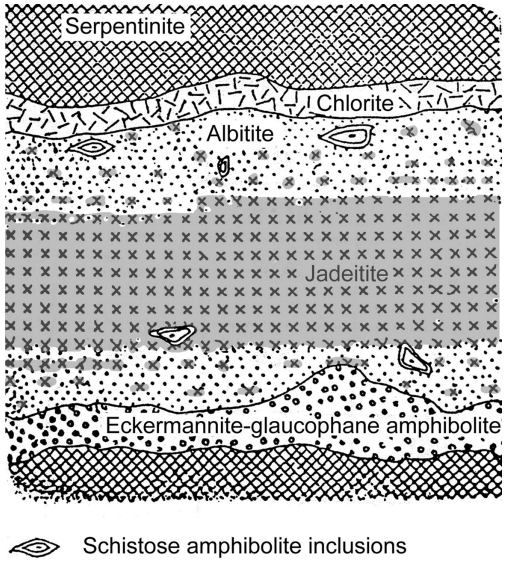

FIG. 11. Diagram of contact relationships of the jadeitite "dike" at Tawmaw, Burma (Myanmar); after Bleeck (1908, Fig. 3).

In Guatemala, the jadeitite occurrence north of the Motagua fault, which is the North American–Caribbean plate boundary, has been described in detail (Harlow, 1994). There, jadeitite occurs as boulders up to 5 m across in drainages and as dismembered tectonic blocks, perhaps 10 m in diameter, in antigorite serpentinite mélanges (Fig. 12). The jadeitite blocks show cataclastic to sheared textures that are cut by coarser-grained veins of undeformed jadeitite. A major post-veining event is albitization; complete replacement of jadeitite by albitite typically occurs toward the boundary of a block with serpentinite. The jadeitite-serpentinite contact zone consists of concentrically foliated blackwall mineralogy (actinolite + clinochlore ± talc) a few cm to perhaps a meter thick, penetrated by centimeter-to decimeter-wide bundles of acicular actinolite aligned radial to the block. Associated tectonic blocks include garnet amphibolite, zoisitized garnet amphibolite, omphacite-taramite metabasite, albite-phengite±zoisite rock, and silexite interpreted as metachert.

Jadeitites have recently been found south of the Motagua fault in the drainage of the Río El Tambor, Jalapa Dept. (Seitz et al., 2001; Harlow et al., 2003b). Likewise found as tectonic blocks in a belt of serpentinite-(antigorite)-mélanges, the jadeitites often contain conspicuous phengitic muscovite and do not show extensive albitization or associated albitites and zoisite-mica-albite rocks. Other HP/LT blocks include abundant lawsonite-eclogite, glaucophane eclogite, omphacite-glaucophane rock, and pumpellyite-jadeite rock (Sisson et al., 2003).

At Clear Creek, in the New Idria serpentinite body of California, adjacent to the San Andreas fault, Coleman (1961) described both jadeitite veins in albite-crossite-acmite-stilpnomelane schist and

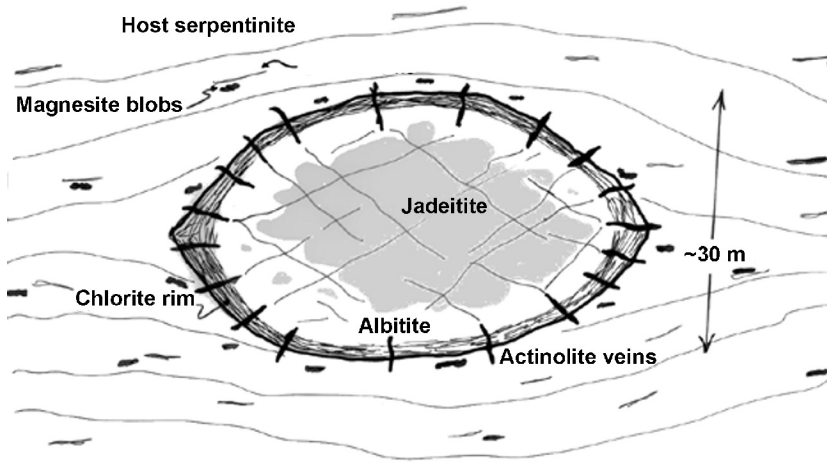

FIG. 12. Diagram of reconstructed zoning pattern for tectonic blocks of jadeitite on north side of Motagua River in Guatemala; from Harlow (1994, Fig. 2).

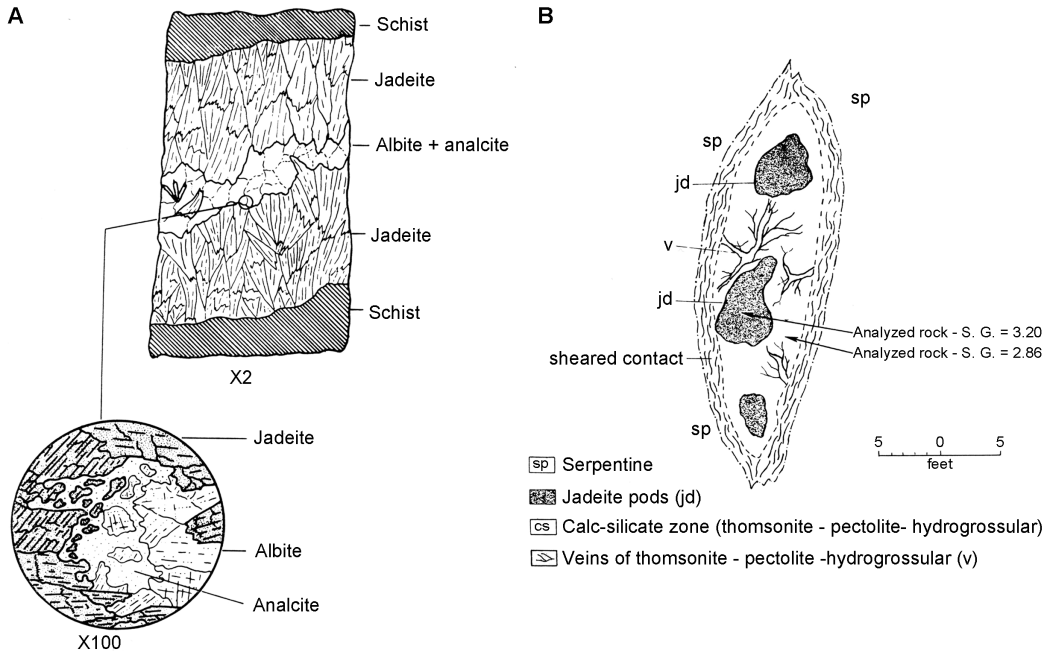

FIG. 13. A. Sketch of jadeite vein in albite-crossite-acmite-stilpnomelane schist showing relationships between jadeite, albite, and analcime; from Coleman (1961, Fig. 5). B. Geological sketch-map of pod-like jadeitite body, locality no. 3, (105-RGC-58); from Coleman (1961, Fig. 6).

jadeitite pods surrounded by calc-silicate carapaces within tectonized serpentinite. Coarse jadeite veins that cut the schist terminate against veins of albite + analcime; albite veins that contain pectolite + thomsonite cut the coarse jadeite veins (Fig. 13A). Jadeitite pods within lenses of calc-silicate rock within sheared serpentinite are up to 3 m in diameter (Fig. 13B). The monomineralic jadeitite pods are cut by veinlets of zeolite minerals ± biotite and clots of native copper. The calc-silicate lenses consist of thomsonite + pectolite ± hydrogrossular; a 2 cm thick boundary that contains both jadeitite and calc-silicate minerals separates the two rock types (Fig 13B). Contacts between the pods and serpentinite consist of sheared, glassy appearing antigorite around chrysotile cores, which gives way to earthy chlorite and then to a zone of calcsilicate minerals like those within the pods, but which also contains bands of titanite and patches of aragonite.

In the Kotaki district, near Itoigawa, Niigata Prefecture, Japan, at the boundary between the Sangun and Hida metamorphic terranes and adjacent to the Itoigawa-Shizuoka Tectonic Line, Iwao (1953), Shidô (1958), and Chihara (1971) described jadeitite, albite-jadeite rock, and albitite blocks eroded from sheared serpentinites and exposed in the Kotaki and Omi gawa (rivers). The jadeitite blocks are up to 4 m in diameter. Zoning patterns from the early literature described a core of albitite (± quartz), up to ~1 meter diameter, surrounded in turn by white jadeitite, which becomes greener farther from the core, then ~10 cm of jadeite-actinolite ± phlogopite rock and a contact zone/rim of massive actinolite ± chlorite ± prehnite. Veins of xonotlite, pectolite, and other secondary minerals cut both jadeitite and albitite. A personal visit (GEH) and observations by T. Tsujimori (pers. commun., 2003) have failed to identify the albitite cores in blocks. Rather, these are interpreted as a zone or layer of albitite. On the basis of petrographic observation, Tsujimori (pers. commun., 2003) interpreted the albitite to be an alteration product of jadeitite.

Three well-documented jadeitite localities occur in Russia and Kazakhstan. In the ophiolite belts of West Sayan (Khakassia, Russia) jadeitites, albitized

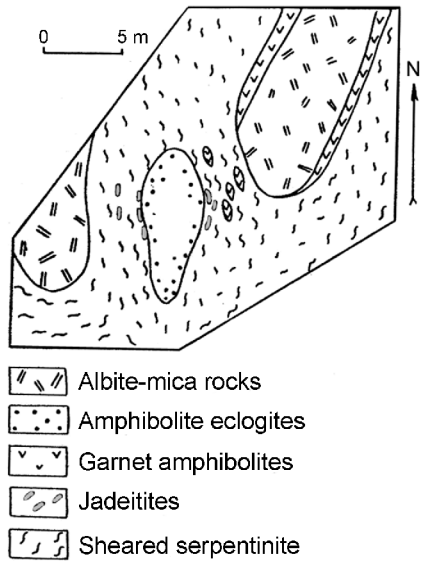

FIG. 14. Relationship of jadeitites to eclogite and mica and albite-mica rocks in Borus mélange, Khakassia (West Sayan), Russia. Figure 6 from Dobretsov (1963).

jadeitites, albitites, eclogites, and glaucophane schist inclusions were described from the Borus serpentinite mélange by Dobretsov (1963; Dobretsov and Tatarinov, 1983). Jadeitites occur as pod-shaped bodies, which in one area are associated with eclogite bodies (Fig. 14), with cores of coarse jadeite and margins of omphacite + amphibole ± phlogopite. Later alteration phases include albite, analcime, Ac- + Ko-rich omphacite, actinolite, mica, and chlorite.

At Itmurundy, near Lake Balkhash, Kazakhstan, Moskaleva (1962), Dobretsov and Ponomareva (1965), Kovalenko and Sviridenko (1981), and Ermolov and Kotelnikov (1991) described a complex association of numerous rocks with the Kenterlaus ultramafic massif. Jadeitites occur as drop-shaped bodies along with granitoids, gabbroic rocks (or altered equivalents), and other metasomatic rocks in serpentinite mélange. Three variations of jadeitite are present: white-to-light grey marble-like rock (typically as cores), a dark grey type (some as an intermediate stage), and bright green jadeitite. All display varying degrees of brecciated and cataclastic structures. Near contacts with serpentinite are assemblages of albite, analcime, natrolite, tremolite, veins of garnet(?) and green mica, and at the contact is a blackwall assemblage of chlorite + actinolite + serpentine (Fig. 15). Albitites typically contain relict fragments of jadeite with muscovite (phengite?), tremolite, rare omphacite, titanite, and rutile. Associated with these albitites, which are interpreted to be altered jadeitites, are quartz-albite, quartz-amphibole, and quartz-dominant rocks.

Jadeitite textures and mineralogy

The textures of jadeitites are complex, but invariably reflect growth from a fluid, upon which may be superimposed resorption by subsequent batches of fluid, recrystallization during deformation, mylonitization or combinations of all these features. Evidence for crystal growth from fluids vary from small areas of (former) cavity filling with well formed, typically zoned jadeite crystals, to

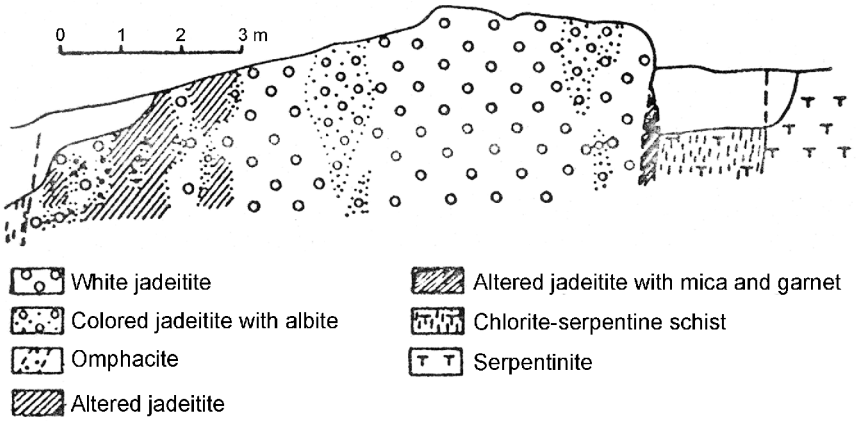

FIG. 15. Cross section of a body of jadeitite in the Kenterlaus ultramafic massif. After Dobretsov and Ponomareva (1965, Fig. 13).

incipient veining, to rocks that appear to be entirely veins. Oscillatory zoning (obvious in cathodoluminescence—CL) is common in jadeite grains from veins (Fig. 16). Deformation features include fractured and partially recrystallized granoblastic grains, to mylonitic textures (Fig. 17).

Minerals that coexist with primary jadeite include sodic amphibole (pargasite-magnesiokatophorite-glaucophane to nyböite and eckermannite in Myanmar; Mével and Kiénast, 1986; Harlow and Olds, 1987, Shi et al., 2003), sodic actinolite (in Japan; Chihara, 1971), and mica (phengite and/or paragonite and preiswerkite in Guatemala; phengite and phlogopite in Japan; phlogopite in the Polar Urals [Dobretsov and Ponomareva, 1965]) ± albite, zoisite, allanite, titanite, rutile, zircon, apatite, chromite, pyrite, and graphite (see Table 3 for a more specific list). Late-stage enrichment of Ba is reflected by the crystallization of banalsite and cymrite in Myanmar (Harlow and Olds, 1987) and in Guatemala (Harlow, 1994), Ba-Ti-silicate in Kazakhstan (Ermolov and Kotelnikov, 1991) and barian phengite in Guatemala (Harlow, 1995). Late-stage enrichments of Sr are seen in the formation of stronalsite at Oosa-cho, Japan (Kobayashi et al., 1987), itoigawaite (the Sr equivalent of lawsonite; Miyajima et al., 1999), rengeite (Miyajima et al., 2001), and matsubaraite (Miyajima et al., 2002) at Itoigawa, Japan, and strontian zoisite (Harlow, 1994) in Guatemala.

Primary jadeitite generally lacks quartz, although the southern jade belt (near Jalapa) in Guatemala has yielded both a quartz-rutile-jadeitite rock (Smith and Gendron, 1997) and quartz jadeitite (Harlow et al., 2004). The quartz-bearing "jadeitite" from Turkey described by Okay and Kelley (1994) and Okay (1997, 2002) occurs as bands in blueschist-facies metapelites and metapsammites, and appears to be a completely different kind of rock type than serpentine-hosted ones. The Jalapa belt of Guatemala also contains rocks with the assemblages pumpellyite + jadeite, quartz + jadeite, and lawsonite + jadeite.

Albitites are a common feature of the jadeitite occurrences, as a boundary zone or with a texture indicating replacement of primary jadeitite; some have been interpreted as cores of blocks. Albitites are described to be an intimate part of the lithologic setting of jadeitite in Myanmar, Guatemala, the Polar Urals, Kazakhstan, Khakassia, and Japan. Albitites may contain relict jadeitite: (1) in a reaction texture with albitite phases; (2) along with omphacite-diopside or actinolite, which outline replaced jadeite grains; or (3) without visible replacement textures of jadeite (described in the Russian literature as "apojadeitites"). The constituents of albitite, which probably represent alteration products or relics of jadeitite phases, as well as an entire secondary albitite suite, include omphacitic-to-diopsidic pyroxene, analcime, zoisite, taramite, actinolite, clinochlore, titanite, natrolite, pectolite, xonotlite, prehnite, zoisite (some as the thulite variety), calcium carbonate, apatite, graphite, and quartz (Table 3). Quartz does not occur in contact with relict jadeite in albitites, a strong indication that these rocks form outside the stability field of quartz + jadeite. Albitite has been described as cores in jadeitite blocks from Itoigawa, Japan (Iwao, 1953; Shidô, 1958; Chihara, 1971) and from Myanmar (Chhibber, 1934) but not in sufficient context with actual totally surrounding jadeitite to establish albitite as a core lithology.

P-T conditions

Estimating P-T conditions for a rock that is most commonly nearly monomineralic necessarily relies on small variations of composition, associated minerals that are sparse and not developed in every jadeitite locality, and techniques other than phase equilibrium considerations, e.g. coexisting rocks. Harlow (1994) used the reactions Anl = Jd + H_2O, Ab = Jd + Qtz, and 4 Lw + 2 Jd = Ab + Pa + 2Cz + $6H_2O$ (with lowered activities of some components) to limit the upper P-T stability of quartz-free jadeitite to ~14 kbar, ~ 450°C (Fig. 18). The relatively T-insensitive nature of the former two reactions essentially precludes estimation of a lower-T limit for jadeitites. Fluid inclusion data reported by Johnson and Harlow (1999) for Guatemalan jadeitite yield a lower-T limit of ~272°C. These authors also calculated T based on the fractionation of ^{18}O between albite and muscovite, which yields T = 327 ± 50°C for an albitite, and between jadeite and albite, for T = 401 ± 50°C; five ^{18}O temperatures for albite-muscovite pairs range from 283° to 302°C (Johnson and Harlow, 1999). Sorensen et al. (2003) measured $\delta^{18}O$ for two jadeite-albite pairs from Burmese jadeitite, which yield T from 300° to 400°C. The presence of jadeite provides a minimum pressure constraint for jadeitites. However, the realizations that jadeitite vein formation requires $P_{H2O} = P_{total}$ and the veins lack quartz, this value is only P > 5–6 kbar (i.e., corresponding to the reaction Jd + W = Anl), not P > 8–11 kbar (i.e., corresponding to the

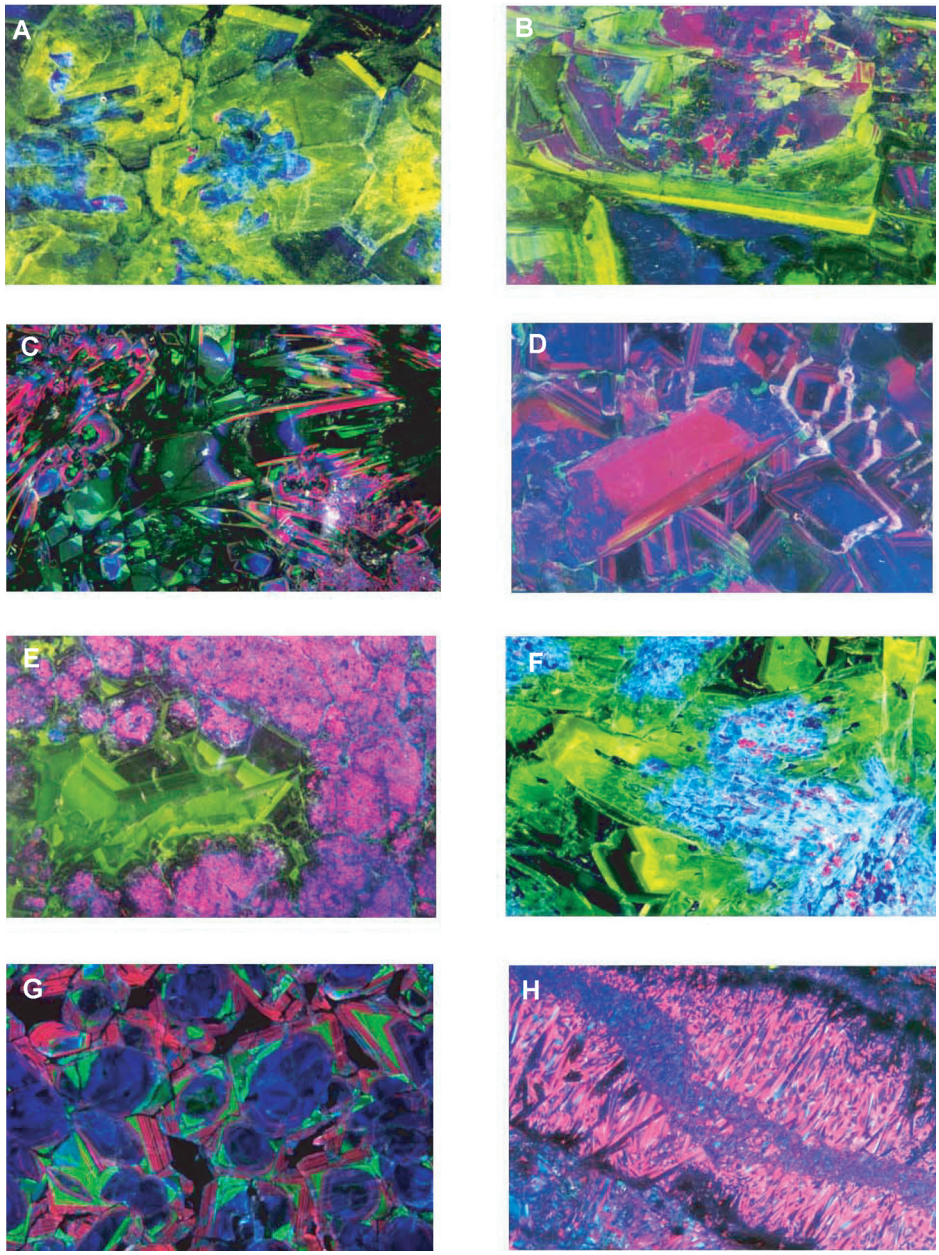

FIG. 16. Cathodoluminesence images of jadeitites. Vertical dimension of all images ~1mm. A. AMNH Specimen 104278, Ketchpel River, Polar Ural Mtns., Russia. B. NMNH Specimen 112701, Myanmar. C. AMNH Field Number 01GSn6-13 (Virginia Sisson), Guatemala. D. NMNH Specimen 94303, Myanmar. E. AMNH Field Number MVJ84-9D (George Harlow), Guatemala. F. NMNH Specimen 105860, Japan. F. AMNH Field Number MVE02-3-1 (Sorena Sorensen), Guatemala. G. NMNH Specimen 113778-1, California. All specimens irradiated at conditions of 20kV and 0.5 mA. Images C and G were collected by an Olympus CCD using Magnafire 2.0 software; the others are scanned emulsion images. The images show the growth of extremely idioblastic grains, oscillitory zoning, and apparent infilling of fluid-filled spaces; images A, B, and F also show apparent resorption and overgrowth features. Image H also shows grain-size reduction and the entrapment of brecciated vein-forming grain fragments along a sheared surface that cuts an earlier-formed vein.

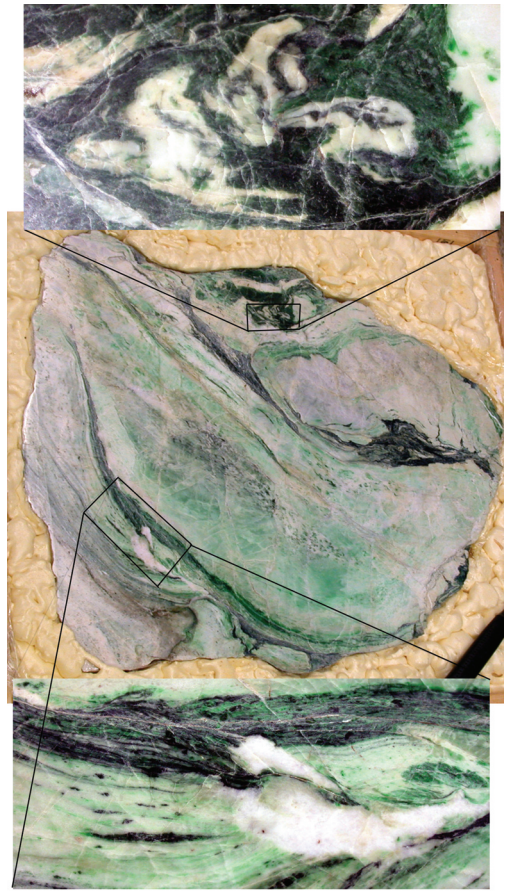

FIG. 17. A sectioned jadeitite boulder showing nodular core of white or light green coarse jadeitite surrounded by finely cataclastically folded to mylonitic banded green (inset at bottom, 14 cm across) and white jadeite with black amphibole fels demarking earlier boundary, all demonstrating considerable deformation, including fine brittle deformational folding (inset at top, 7.3 cm across). AMNH 109752, Jade Tract, northern Myanmar, largest dimension is 74 cm.

reaction Jd + Qtz = Ab) for the above temperature estimates (Fig. 18).

The P-T conditions of jadeitite formation can also be constrained by the serpentinite host rocks and perhaps by the phase assemblages of the tectonic blocks found with jadeitite in the mélange units, provided the mélange does not contain blocks that represent a variety of P-T conditions (e.g., Cloos, 1986). As noted above, many *in situ* jadeitite bodies are hosted by serpentinite that consists of antigorite (± brucite) adjacent to the jadeitite. The metamorphic rocks associated with jadeitite, either adjacent to the host serpentinite body or as mélange blocks within it, include blueschist-facies metabasites (Myanmar—Chhibber, 1934; Goffe et al., 2000; Guatemala—Harlow, 1994; Harlow et al., 2004, Japan—Shidô, 1958; Chihara, 1971; Komatsu, 1987). Rutile mantled by titanite is characteristic of jadeitites and is also ubiquitous in accompanying metabasites, suggesting blueschist-facies retrogression of higher-T assemblages.

The presence of lawsonite and/or pumpellyite in one group of jadeitites of Jalapa, Guatemala, and Qtz + Jd in another, respectively, imply conditions of lower temperature for the former and silica saturation at possibly higher pressure for the latter (Fig. 18). In serpentinite-matrix mélanges that yield quartz-jadeitites (and more ordinary looking phengite jadeitites) lawsonite eclogites are also present, which represent very high-pressure, low-temperature (VHP/LT) conditions (20–25 kbar, ~400–550°C; Sisson et al., 2003). Thus, jadeitites appar-

TABLE 3. Mineral Assemblages Characteristic of Jadeitites

Location	Assemblage
Myanmar—Tawmaw, Lonkin, etc.	Primary: Jadeite, omphacite, sodic amphiboles, chromite, kosmochlor, zircon, graphite Secondary: Albite, analcime, banalsite, cymrite, clinochlore
Guatemala 1—North of MFZ (Maya Block)	Primary: Jadeite, omphacite, albite, analcime?, paragonite, phengite, preiswerkite, zircon, rutile, titanite, zoisite, allanite, apatite, graphite, pyrite. Secondary: Analcime, albite, nepheline, taramite, titanite, banalsite, cymrite, celsian, K-spar, clinochlore
Guatemala 2—South of MFZ (Chortís Block)	Primary: Jadeite, omphacite, phengite, quartz, lawsonite, pumpellyite, pectolite, zircon, rutile, titanite, apatite, allanite Secondary: Albite, zoisite, vesuvianite, quartz, tremolite, diopside, cymrite
Japan—Itoigawa	Primary: Jadeite, omphacite, albite, eckermannite-barroisite-taramite, titanite, rutile, zircon, actinolite, clinochlore, quartz? Secondary: Analcime, natrolite, lamprophyllite, zoisite (thulite), xonotlite, pectolite, slawsonite, tausonite, rengeite, matsubaraite, itoigawaite, Sr-apatite
California—Clear Creek, New Idria, California	Primary: Jadeite, omphacite, albite?, native copper? Secondary: Albite, natrolite, pectolite, analcime, native copper
Russia—Ketchpel, Polar Urals	Primary: Jadeite Secondary: Omphacite, albite, phlogopite, tremolite, analcime, natrolite, phillipsite
Kazakhstan—Itmurundy	Primary: Jadeite, omphacite, titanite, rutile, albite, graphite, magnetite, chromite, pumpellyite? Secondary: Albite, analcime, natrolite, tremolite, green mica (phengite?), benitoite? (a Ba-Ti-silicate)
Khakassia—Yenisey River (Borus mélange)	Primary: Jadeite, omphacite, "hornblende," phlogopite, rutile, garnet? Secondary: Albite, Ac+Ko-rich omphacite, epidote, Na-actinolite, analcime, chlorite, carbonate

ently form over a range of P-T conditions, from the lawsonite-eclogite- to blueschist-facies. Jadeitite bodies and the units that host them appear to reflect subduction-zone metasomatic processes as well as the tectonics that exhume them in serpentinite-matrix mélanges.

The outcrop appearance of jadeitite bodies, especially the well-known locality at Tawmaw, Myanmar were interpreted by early workers to be tabular masses ("dikes"; Fig. 11). This observation, combined with the restriction to occurrence in bodies of faulted serpentinite (or later, to serpentinite matrix mélange), probably led to the notion that jadeitite represented metamorphosed and extremely metasomatized veins or dikes of albite granite (trondjemite) that had intruded peridotite, then gained Na_2O and lost SiO_2 (e.g., Bleeck, 1908; Chhibber, 1934). Similar interpretations for jadeitite from the Polar Urals, Russia and Itmurundy, Kazakhstan were argued by Dobretsov and Ponomareva (1965), although the protoliths were described as granitoids and leucogabbros, in the latter case. Transforming a plagiogranite (or a quartz keratophyre) into a jadeitite requires a far more complex mass balance than this model implies (e.g., Harlow, 1994). As more isolated blocks of jadeitite,

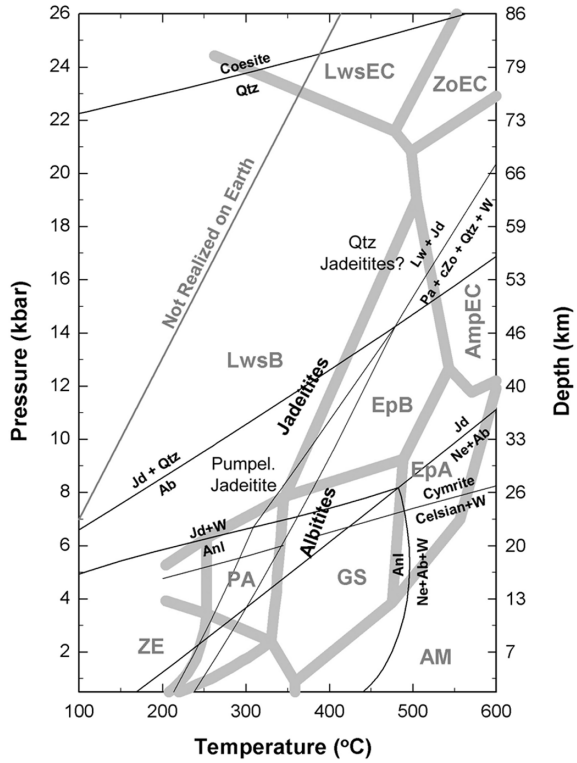

FIG. 18. Pressure-temperature diagram for jadeitites. A petrogenetic grid is shown for metabasites that uses facies boundaries from Peacock (1993) at pressures to about 20 kbar and Katayama et al. (2001) at higher pressures. Reactions are limits for jadeitite and albitite formation (Harlow, 1994).

and associated rounded mafic blocks, but no felsic ones, were found and described, the interpretation turned to wholesale replacement of tectonic mélange blocks of original leucocratic igneous or sedimentary provenance (e.g., Chhibber, 1934; Dobretsov and Ponomareva, 1965; McBirney et al., 1967; Silva, 1967, 1970; Bosc, 1971). Coleman (1961) drew similar conclusions at New Idria, California, although at that locality, jadeitites occur in two settings, as described above. Hirajima and Compagnoni (1993) described jadeite-garnet-phengite-coesite fels from the southern Dora Maira massif, Western Alps, which is a layer in a HP orthogneiss sequence. Felsic metasedimentary rocks have different mass balance issues than do plagiogranites, but again, a formidable number of components must be added and subtracted from either metagraywacke or metapelite to effect a transformation to jadeitite. Based on a concentric zonation of bodies in serpentinite mélange consisting of eclogite cores, surrounding omphacite rock, and small jadeitite bodies surrounding them (Fig. 14), Dobretsov (1963) proposed that jadeitites in West Sayan replaced eclogite blocks. Compagnoni and Rolfo (2003) have observed patterns of rutile grains, which they interpreted to be remnants of a boudinaged vein of basalt or trondhjemite, in a newly discovered jadeitite at Punta Rasciassa, Italy. Like all of the other proposed protoliths, mafic rocks have severe mass balance problems, in this case because of their large Mg, Fe, and Ca contents, with no obvious sinks in serpentinizing peridotite (e.g., Harlow, 1994).

Other lines of evidence suggest that these genetic models should be considerably modified. We have employed CL imaging, a method that utilizes the effect small changes in minor or trace-element concentrations have upon the luminescence of jadeite crystals that dramatically manifests their growth zoning. We have studied >100 jadeitite specimens from all major localities and found no relics of protolith replacement textures, only earlier crystal-

lized generations of jadeite (e.g., Harlow, 1994; Sorensen and Harlow, 1998, 1999, 2001). With CL, crystals of jadeite in jadeitites are shown to be cryptically to rhythmically zoned (Fig. 16); in petrographic examination, they are seen to contain two-phase aqueous fluid inclusions. Together, these observations support an interpretation of direct crystallization from an aqueous fluid. Although many jadeitites show evidence for multiple deformation, recrystallization, and deposition events, the latest episode of crystallization is invariably via vein and/or crack systems within the rocks. Because low silica activity must be maintained in order to form quartz-free jadeitite, a genetic relationship with serpentinizing fluid in fractures is implied, with minimal involvement of metasomatic replacement of a protolith. This interpretation obviously conflicts with the model of Dobretsov (1963) and observations of Compagnoni and Rolfo (2003) at Punta Rasciassa; however, we regard these two examples of metasomatic replacement as exceptions to the majority of jadeitite occurrences and samples.

Fluid inclusion salinities and O/H isotopic systematics in jadeitites from Guatemala have been interpreted to indicate the predominance of a seawater-like fluid, entrained during subduction, rather than the product of dehydration of deep metamorphic minerals (Johnson and Harlow, 1999). Similarly, both primary and secondary fluid inclusions in eclogite and garnet amphibolite samples from the Franciscan Complex and Catalina Schist, California, and the Samaná Peninsula, Dominican Republic preserve seawater-like salinities (Sorensen and Barton, 1987; Giaramita and Sorensen, 1994).

Trace element and oxygen isotope studies of jadeitites with SIMS elucidate certain common compositional traits that distinguish between deposits and, yet, indicate that individual grains of jadeite can manifest considerable heterogeneity during growth. Overall trends suggest that some deposits have a strong signature from sediments (perhaps in Guatemala), whereas others may record a significant felsic-igneous component (perhaps Myanmar) (Sorensen and Harlow, 1998, 1999; Sorensen et al., 2003). However, highly variable trace-element zoning in jadeite from a single deposit suggests that diverse fluid compositions are recorded by different jadeitite blocks in the same unit. It is therefore possible that hydrous fluids involved in jadeitite crystallization derive from various sources in the subduction system, and we, the authors, are not in full agreement about those different possible sources, even for the Guatemala jadeitites. One of us (GEH) believes fluid could be derived from dewatering and some shallower dehydration, whereas we both agree that an important fluid source must be devolatilization within a subducting slab at depths that correspond to the blueschist-to-eclogite transition, as well as other more continuous dehydration sources, as argued by Schmidt and Poli (1998). High-pressure experiments indicate fluids in equilibrium with the P-T-x of this transition will be enriched in Na, Al, and Si, all important to potential saturation of jadeite (e.g., Manning, 1998). It seems possible that such fluids, if they enter a depleted ultramafic rock, could produce jadeitite at P-T conditions below the Jd + Qtz = Ab reaction, provided that the SiO_2 activity was insufficient to crystallize albite. Even though jadeitite from Guatemala shows important tracers from a sedimentary source, and a seawater signature may be indicated (Johnson and Harlow, 1999), it is not clear how a relatively Na-, Al-, Si-rich fluid can be produced solely by dewatering of sediments.

One study of the interaction of originally basaltic mafic blocks in an ultramafic matrix indicates that the blocks can be stripped of many elements during subduction-zone hydration. In the amphibolite unit of the Catalina Schist, large amounts of both SiO_2 and H_2O were added to an ultramafic mélange that contains numerous mafic meta-igneous blocks (Bebout and Barton, 2002). Much of the SiO_2 that metasomatized parts of the ultramafic mélange matrix was derived from the blocks. When H_2O was introduced to a system that probably originally consisted of eclogite + peridotite, mafic blocks reacted with the ultramafic matrix, forming rinds rich in SiO_2 and MgO at block-host rock contacts. Then, parts of rinds were stripped mechanically from the blocks by deformation, which was probably enhanced by the local presence of H_2O. The rinds further reacted with the host rocks to redistribute SiO_2 more widely within the matrix, to yield chlorite ± actinolite schists.

Associated serpentinite

As noted above, some primary jadeitite bodies are adjacent to serpentinite that consists primarily of antigorite, whereas other serpentinites in the serpentinite mélange belts may consist of chrysotile ± lizardite. In fact, this relationship has been noted for the localities at Punta Rasciassa, Italy (Compagnoni and Rolfo, 2003; R. Compagnoni, pers. comm., 2003); Tawmaw (Shi et al., 2001, 2003) and Nant

Maw Mine #109 (GEH) in the Jade Tract, Myanmar; as well as Guatemala (e.g., Sisson et al., 2003).

The mode of occurrence of antigorite in jadeitite-bearing serpentinite mélanges is a clue to the earliest fluid-rock history that the jadeitite-serpentinite system records. In the system MgO-SiO_2-H_2O, chrysotile forms antigorite + brucite at P-T conditions that range from 250°C at 1 bar to ~175°C at 20 kbar; Al-free lizardite is modeled to have a P-T stability that overlaps the lower-T portion of P-T stability range of antigorite (Evans et al., 1976; Berman et al., 1986; O'Hanley, 1996). Thus, antigorite serpentinite found adjacent to jadeitite bodies is likely a product of the hydration of virtually unserpentinized ultramafic rock at relatively high temperatures (i.e., 300–400°C) by jadeitite-forming fluids, and therefore represents the early, HP/LT history of jadeitite-bearing serpentinite mélange. A low degree of serpentinization in ultramafic rock hosting jadeitite would explain the lack of quartz in jadeitite, inasmuch as the ultramafic mars will act like a sponge for the fluid and silica in it during serpentinite formation. The presence of late Ca-enrichment in and around jadeitite bodies, as well as the introduction of Cr-richer jadeite and Cr-bearing minerals into many jadeitites via late-stage veining (and tectonic admixing) suggests formation of this composition of jadeite after a considerable degree of serpentinization has occurred. At this point, the "sponge effect" of the ultramafic rock has decreased, and ultramafic clinopyroxene and primary spinel break down. Their components are released into the fluid in the serpentinite, which could mix with the vein fluid. This is consistent with the observation that serpentinite-hosts of jadeitites contain few, if any, relict peridotite minerals (e.g., Coleman, 1961; Harlow, 1994).

Chrysotile and lizardite clearly reflect lower temperatures of serpentinite genesis than is consistent with the T inferred for jadeitite formation. These may form at the expense of antigorite, particularly in fluid-saturated shear zones during exhumation. Alternatively, some fraction of the low-T serpentine minerals may be relicts of pre-subduction hydration within the oceanic crust of the downgoing slab (e.g., Carlson and Miller, 1997) that are exposed in different slices of the ultramafic massif. Also, serpentinization of peridotite that was not exposed to fluids at depth may take place near the Earth's surface, following the bulk of the exhumation. At present, no data exist that can discriminate among these hypotheses for the presence of low-T serpentine in jadeitite-bearing serpentinite-matrix mélange.

Mode of formation and tectonic implications

Solubility experiments related to the blueschist-to-eclogite transition (Manning, 1998) indicate that dewatering of the hydrated basaltic component of subducting slab produces Na-Al-Si–rich fluids, which should be capable of forming jadeitite within an active subduction zone. Fluid flow into faulted peridotite, which could have originated as fragments of the mantle wedge or slices of basal ocean crust incorporated into subduction zone mélanges, evidently promotes the crystallization of jadeitite veins. The rheological contrast between the competent veins and their serpentinite matrix suggests that deposition of successive generations of jadeite on previous ones might be enhanced as the veins became preferred locations for deformation and fluid flow during serpentinization, ductile material flow, and brittle faulting (Fig. 19). Fluid that traveled down both P and T from its source would tend to crystallize jadeitite, whereas a down-P, up-T flow path could form albitite (e.g., Bebout and Barton, 1993; Harlow, 1994; Bebout et al., 1999). The fluid flow path and crystallization sequence could also be affected by the mode of ascent of serpentinite, which is documented to rise rapidly and diapirically through subduction zone forearcs (Fryer et al., 1999). The modern tectonic setting of jadeitites and hosting serpentinites along transform-type faults may indicate another aspect of the environment of emplacement, which has been interpreted in terms of an oblique collision with buoyancy, parallel stretching at the plate margin, and late thrusting for the Guatemala occurrences (Harlow et al., 2004)

The textural evolution of jadeitites worldwide indicates multiple styles of grain growth, and in some cases the alternation of static crystallization, hydrofracture, resorption, and grain size reduction by ductile deformation. Cycles of jadeite crystallization begin with near–end member compositions, and evolve to contain up to 10% diopside solid solution. More than one of these sequences is recorded by some jadeitite samples. Abundant growth bands, seen both in CL and backscattered electron imaging or X-ray mapping with the scanning electron microscope, document fractures that have been infilled by later jadeite (see Fig. 16). Brittle deformation, probably in the form of hydrofracture, apparently allows fluid access to jadeitite masses. Some jadeitites show evidence for grain-boundary fluid perco-

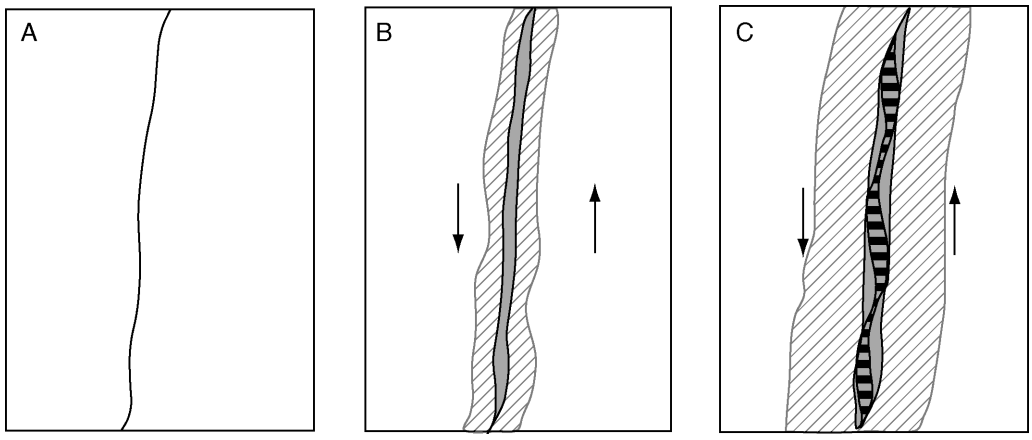

FIG. 19. Diagram of model for formation of jadeitite. A. Fracture forms in peridotite. B. Shear motion opens portions of fracture to permit jadeite-saturated vein fluid to deposit jadeitite (shaded) in the fracture and fluid infiltration into the peridotite commencing serpentinization (diagonal hachures). C. Successive fracturing focuses on existing brittle jadeitite, allowing precipitation of additional jadeitite (horizontal bars) crystallization in the vein system and further fluid infiltration serpentinization of peridotite.

lation, seen in a new generation of jadeite that decorates an aggregate of grains with different compositions. Other specimens contain shear zones that evidently comminuted grains by orders of magnitude. A few jadeitite grains show resorbed cores of one composition, surrounded by growth-zoned, idioblastic jadeite. Jadeitites obviously testify to a dynamic environment of formation (Fig. 17).

One of the puzzling features of jadeitites is the description of albitite cores in some blocks. All jadeitites we have examined, including those from localities where albitite cores are documented (Itoigawa and Myanmar), have clear textural evidence of crystallization from a fluid, so we are fairly certain they are not metasomatized albitite. The critical difference between these two lithologies in serpentinite mélanges is their silica content, because otherwise jadeite and albite can be stable over a sizable range of P-T conditions, between the Anl = Jd + H_2O and Ab = Jd + Qtz reaction boundaries (see Fig. 18); a metamorphic facies change is not necessarily required. Most jadeitite occurrences feature albitite as both an alteration product of jadeitite and a separate lithology subsequent to jadeitite. Thus, in most of the occurrences, silica activity rose to albite saturation after jadeitite formed, rather than before.

However, it isn't clear whether this depends on local effects of serpentinization upon fluids, or a combination of primary fluid compositions and their P-T-x paths. Some tectonic blocks cut by jadeitite are similar to albitite, e.g., the schists at Clear Creek, California (Coleman, 1961), but the Itoigawa, Japan deposits lack schist-like or other felsic blocks, containing only albitites. We are left to conclude that the cases cited with albitite cores represent either misidentified tectonic inclusions that somehow were surrounded by jadeitite crystallizing from a fluid, an unusual example of albitite crystallization from a fluid prior to jadeitite within an ultramafic, or something other than a core-to-rim relationship that may have been physically created by deformation. T. Tatsumi (pers. comm., 2003) has recently studied the albitite-jadeitite relationships at Itoigawa, and confirmed that albitite only appears to be at the cores of some jadeitites but it is actually texturally later. So, further studies of these samples are indeed required.

The rarity of jadeitite within blueschist belts means that the conditions for its formation, the subsequent P-T and fluid regimes to which it is exposed, and the tectonics appropriate for emplacement and preservation rarely occur. The apparent association of jadeitite-bearing serpentinite mélange with major plate boundary zones (PBZ) suggests more than just diapiric rise of host serpentinite may be required for preservation. Recent studies by ourselves and our co-workers (Harlow et al., 2003b, 2004) suggest that along the Motagua fault zone, at least some components of the

mélanges ascended from ~60–80 km depths without experiencing thermal metamorphism (also, evidence for substantial extension parallel to the PBZ is present.) Thrusting plus erosion (Harlow et al., 2004), which seem to be a feature of oblique collision converting into a strike-slip PBZ (Avé Lallemant and Guth, 1990), appear to have effected final stages of uplift. Evidence for similar tectonic processes is present in Myanmar and Japan. If this particular concatenation of syn- and post-subduction tectonic processes is required to exhume jadeitite, their paucity is not particularly surprising.

Conclusions

Many nephrite and all jadeitite deposits record fluid-rock interactions associated with serpentinizing peridotite at depths from >50 km to the near surface in convergent margin environments. Although the formation of large bodies of jadeitite ought to be fairly common, its exhumation and preservation are evidently relatively rare. These processes may require sequences of tectonic conditions that are uncommon. Both jadeitite and nephrite contain evidence for fluid-rock interactions over a large range of P-T-x fluid conditions. As such, they have recorded convergent margin processes that are not well represented by other rock types affected by subduction zone devolatilization. Jade, a material long cherished by many human cultures, is thus petrotectonically significant because of what it can relate about mass transfer by fluids in both subduction and obduction environments of convergent margins. Finally, Bob Coleman's studies of jade in California and New Zealand, and his work on tectonic inclusions in serpentinites have formed our fundamental inspiration for this paper, and we congratulate him on the occasion of his 80th birthday.

Acknowledgments

The authors are particularly grateful for translations of Russian literature made by Nellie Shulova, samples from Janet Douglas, and financial support of jade research by a grant to GEH by the Frohlich Charitable Trust; the Astor Expedition Fund in the Department of Earth and Planetary Sciences, AMNH; the American Museum of Natural History; and Michael Scott. SSS acknowledges the support of the Sprague Fund, Smithsonian Institution, and the assistance of Tim Gooding and Tim Rose in the preparation of specimens for CL at the Smithsonian's National Museum of Natural History. Moral and intellectual support has been provided by our fellow jade-study colleagues: Virginia B. Sisson, Hans Ave Lallemant, Russell Seitz, Charles Mandeville, Sidney Hemming, Hannes Brueckner, and Mauricio Chiquin. Constructive reviews by Mark Cloos and Aley El-Shazly were very helpful. Most recently the authors are grateful for support from NSF through grant EAR-0309320.

REFERENCES

Avé Lallemant, H. G., and Guth, L. R., 1990, Role of extensional tectonics in exhumation of eclogites and blueschists in an oblique subduction setting, northwestern Venezuela: Geology, v. 18, p. 950–953.

Avé Lallemant, H. G., Harlow, G. E., Sorensen, S. S., Sisson, V. B., Kane, R. E., Han Htun, and Myint Soe, 2000, The Nansibon Jade Mines, Myanmar: Structure and Tectonics: EOS (Transactions of the American Geophysical Union), v. 81, no. 48, p. F1108.

Bauer, M., 1895, On the jadeite and other rocks from Tawmaw in Upper Burma: Records of the Geological Survey of India, v. 28, no. 3, p. 91-105 (translated by F. Noetling and H.H. Hayden)[as reprinted in Bulletin of the Friends of Jade, v. 9, p. 13–22.]

Bebout, G. E., and Barton, M. D., 1993, Metasomatism during subduction: Products and possible paths in the Catalina Schist, California: Chemical Geology, v. 108, p. 61–92.

Bebout, G. E., and Barton, M. D., 2002, Tectonic and metasomatic mixing in a high-T, subduction-zone melange; insights into the geochemical evolution of the slab-mantle interface: Chemical Geology, v. 87, no. 1-2, p. 79–106.

Bebout, G. E., Ryan, J. G., Leemanm, W. P., and Bebout, A. E., 1999, Fractionation of trace elements by subduction-zone metamorphism; effect of convergent-margin thermal evolution: Earth and Planetary Science Letters, v. 171, p. 63–81.

Beck, R., 1984, New Zealand jade: Wellington, NZ, A. H. & A. W. Reed, Ltd., 173 p.

Beck, R., 1991, Jade in the South Pacific, *in* Keverne, R., ed., *Jade*: New York, NY, Van Nostrand Reinhold, p. 221–258.

Bender, F., 1983, Geology of Burma: Berlin, Germany, Gebrüder Borntraeger, 293 p.

Berman, R. G., Engi, M., Greenwood, H. J., and Brown, T. H., 1986, Derivation of internally consistent thermodynamic data by the technique of mathematical programming: A review with application to MgO-SiO_2-H_2O: Journal of Petrology, v. 27, p. 1331–1364.

Bleeck, A. W. G., 1907, Die Jadeitlagerstätten in Upper Burma: Zeitschrift für praktische Geologie, v. 15, p. 341–365.

Bleeck, A. W. G., 1908, Jadeite in the Kachin Hills, Upper Burma: Records of the Geological Survey India, v. 36, no. 4, p. 254–285 [as reprinted in the Bulletin of the Friends of Jade].

Bosc E. A., 1971, Geology of the San Agustín Acasaguastlan quadrangle and northeastern part of El Progreso quadrangle: Unpubl. Ph.D. dissertation, Rice University, 131 p.

Brady, J. B., 1977, Metasomatic zones in metamorphic rocks: Geochimica et Cosmochimica Acta, v. 41, p. 113–125.

Bromiley, G. D., and Pawley, A. R., 2003, The stability of antigorite in the systems MgO-SiO_2-H_2O (MSH) and MgO-Al_2O_3-SiO_2-H_2O (MASH): The effects of Al^{3+} substitution on high-pressure stability: American Mineralogist, v. 88, p. 99–108.

Carlson, R. L., and Miller, D. J., 1997, A new assessment of the abundance of serpentinite in the oceanic crust: Geophysical Research Letters, v. 24, p. 457–460.

Chhibber, H. L., 1934, The mineral resources of Burma: London, UK, MacMillan, 320 p.

Chihara, K., 1971, Mineralogy and paragenesis of jadeites from the Omi-Kotaki area, Central Japan: Mineralogical Society of Japan, Special Paper 1, p. 147–156.

Cloos, M., 1986, Blueschists in the Franciscan Complex of California: Petrotectonic constraints on uplift mechanisms, *in* Evans, B. W., and Brown, E. H., eds., Blueschists and eclogites, Geological Society of America Memoirs, v. 164, p. 77–94.

Coleman, R. G., 1961, Jadeite deposits of the Clear Creek area, New Idria district, San Benito County, California: Journal of Petrology, v. 2, p. 209–247.

Coleman, R. G., 1966, New Zealand serpentinite and associated metasomatic rocks: Bulletin, New Zealand Geological Survey, v. 76, 102 p.

Coleman, R. G., 1967, Low-temperature reaction zones and Alpine ultramafic rocks of California, Oregon, and Washington: U.S. Geological Survey Bulletin, v. 1247, 49 p.

Coleman, R. G., 1977, Ophiolites, ancient oceanic lithosphere?: Berlin, Germany, Springer Verlag, 229 pp.

Coleman, R. G., 1980, Tectonic inclusions in serpentinite: Archives des Sciences (Société de Physique D'Histoire Naturelle de Genève), v. 33, p. 89–102.

Compagnoni, R., and Rolfo, F., 2003, First finding of jadeite in the serpentinite mélange of Monviso meta-ophiolite, Western Alps [abs.]: The Alice Wain Memorial Western Norway Eclogite Field Symposium, June 21st–28th, 2003, Selje, western Norway, Abstract Vol., p. 37.

Cooper, A. F., 1976, Concentrically zoned ultramafic pods form the Haast schist zone, South Island, New Zealand: New Zealand Journal of Geology and Geophysics, v. 19, no. 5, p. 603–623.

Cooper, A. F., 1995, Nephrite and metagabbro in the Haast Schist at Muddy Creek, Northwest Otago, New Zealand: New Zealand Journal of Geology and Geophysics, v. 38, p. 325–332.

Dobretsov, N. L., 1963, Mineralogy, petrography and genesis of ultrabasic rocks, jadeitites, and albitites from the Borus Mountain Range (the West Sayan): USSR Academy of Sciences (Siberian Branch), Proceedings of the Institute of Geology and Geophysics, v. 15, p. 242–316.

Dobretsov, N. L., 1984, Problem of the jadeite rocks, associating with ophiolites: Mineralia slovaca, v. 16, p. 3–12.

Dobretsov, N. L., and Ponomareva, L. G., 1965, Comparative characteristics of jadeite and associated rocks from Polar Ural and Near-Balkhash Region: USSR Academy of Sciences (Siberian Branch), Proceedings of the Institute of Geology and Geophysics, v. 31, p. 178–243.

Dobretsov, N. L., and Tatarinov, A. V., 1983, Jadeite and nephrite in ophiolites (the example of West Sayan): Novosibirsk, USSR, Nauka Press, 123 p. (in Russian).

Dorling, M., and Zussman, J., 1985, An investigation of nephrite jade by electron microscopy: Mineralogical Magazine, v. 49, p. 31–36.

Douglas, J. G., 1996, The study of Chinese archaic jades using non-destructive X-ray fluorescence spectroscopy: Acta Geologica Taiwanica, v. 32, p. 43–54.

Douglas, J. G., 2003, Exploring issues of geological source for jade worked by ancient Chinese cultures with the aid of X-ray fluorescence, in Jett, P., ed., Scientific study in the field of Asian art: London, UK, Archetype Publications Ltd., p. 192–199.

El-Shazly, A. K., and Al-Belushi, M., 2004, Petrology and chemistry of metasomatic blocks from Bawshir, NE Oman: International Geology Review, v. 46, forthcoming.

Ermolov, P. V., and Kotelnikov, P. E., 1991, Composition and origin of jadeitites of Imurundinsky Melange (northern Balkhash Area): Soviet Geology and Geophysics, v. 2, p. 44–51.

Evans, B. W., Johannes, W., Oterdoom, H., and Trommsdorf, V., 1976, Stability of chrysotile and antigorite in the serpentinite multisystem: Schweizerisches Mineralogisches und Petrographisches Mitteilungen, v. 56, p. 79–93.

Flint, D. J. and Dubowski, E. A., 1990, Cowell nephrite jade deposits, *in* Hughes, F. E., ed., Geology of the mineral deposits of Australia and Papua New Guinea; Vol. 2. Melbourne, Australia, Institute of Mineralogy and Metallurgy, v. 14, p. 1059–1062.

Fryer, P., Wheat, C. G., and Mottl, M. J., 1999, Mariana blueschist mud volcanism; implications for conditions within the subduction zone: Geology, v. 27, no. 2, p. 103–106.

Gabrielse, H., 1990, Cry Lake jade belt, north-central British Columbia: Calgary, Canada, Geological Survey of Canada, Open-File Report 2262.

Gaines, A. M., and Handy, J. L., 1975, Mineralogical alteration of Chinese tomb jades: Nature, v. 253, p. 433–434.

Germine, M., and Puffer, J. H., 1989, Origin and development of flexibility in asbestiform fibres: Mineralogical Magazine, v. 53, p. 327–335.

Giaramita, M. J., and Sorensen, S. S., 1994, Primary fluids in low-temperature eclogites: Evidence from two subduction complexes (Dominican Republic, and California, USA): Contributions to Mineralogy and Petrology, v. 117, p. 279–292.

Goffe, B., Rangin, C., and Maluski, H., 2000, Jade and associated rocks from jade mines area, northern Myanmar as record of a polyphased high pressure metamorphism [abs.]: EOS (Transactions of the American Geophysical Union), v. 81, no. 48, p. F1365.

Gurulev, S. A. and Shagzhiyev, K. Sh., 1973, Geology and conditions of formation of the Param nephrite deposit in eastern Siberia, in: Nonmetallic hyperbasite natural resources: Moscow, USSR, Nauka Press, p. 234–244 (in Russian).

Harlow, G. E., 1994, Jadeitites, albitites, and related rocks from the Motagua Fault Zone, Guatemala: Journal of Metamorphic Geology, v. 12, p. 49–68.

Harlow, G. E., 1995, Crystal chemistry of barian enrichment in micas from metasomatized inclusions in serpentinite, Motagua Valley, Guatemala: European Journal of Mineralogy, v. 7, 9. 775–789.

Harlow, G. E., Hemming, S. R., Avé Lallemant, H. G., Sisson, V. B., and Sorensen, S. S., 2004, Two high-pressure–low-temperature serpentine-matrix melange belts, Motagua Fault Zone, Guatemala: A record of Aptian and Maastrichtian Collisions: Geology, v. 31, no. 1, p. 17–20.

Harlow, G. E., and Olds, E. P., 1987, Observations on terrestrial ureyite and ureyitic pyroxene: American Mineralogist, v. 72, p. 126–136.

Harlow, G. E., Rossman, G. R., Matsubara, S., and Miyajima, H., 2003a, Blue omphacite in jadeitites from Guatemala and Japan: Crystal chemistry and color origin [abs.]: Geological Society of America Abstracts with Program, v. 35, no. 6, [abstract 65497, CD-ROM 254-1].

Harlow, G. E., Sisson, V. B., Avé Lallemant, H. G., and Sorensen, S. S., 2003b, High-pressure, metasomatic rocks along the Motagua Fault Zone, Guatemala: Ofioliti, v. 28, no. 4, p. 115–120.

Hausel, W. D., 1993, Preliminary report on the geology, geochemistry, mineralization, and mining history of the Seminoe Mountains mining district, Carbon Co., Wyoming: Wyoming Geol. Assoc. Guidebook, v. 44, p. 387–410.

Hirajima, T., and Compagnoni, R., 1993, Petrology of a jadeite-quartz/coesite-almandine-phengite fels with retrograde ferro-nyböite from the Dora-Maira Massif, Western Alps: European Journal of Mineralogy, v. 5, no. 5, p. 943–955.

Hockley, J. J., Birch, W. D., and Worner, H. K., 1978, A nephrite deposit in the Great Serpentine Belt of New South Wales: Journal of the Geological Society of Australia, v. 25, no. 5-6; p. 249–254.

Hughes, R. W., Galibert, O., Bosshart, G., Ward, F., Oo, T., Smith, M., Sun, T. T., and Harlow, G. E., 2000, Burmese jade: The inscrutable gem: Gems and Gemology, v. 36, no. 1, p. 2–26.

Iwao, S., 1953, Albitite and associated jadeite rock from Kotaki District, Japan: A study in ceramic raw material: Reports of the Geological Survey of Japan, v. 153, 26 p.

Johnson, C. A. and Harlow, G. E., 1999, Guatemala jadeitites and albitites were formed by deuterium-rich serpentinizing fluids deep within a subduction-channel: Geology, v. 27, p. 629–632.

Karpov, I. K., Chudnenko, K. V. and Suturin, A. N., 1989, Physicochemical modeling of processes of contact-infiltration metasomatism: Transactions of the USSR Academy of Sciences, Earth Science Section, v. 297, p. 189–192.

Katayama, I., Maruyama, S., Parkinson, C. D., Terada, K., and Sano, Y., 2001, Ion micro-probe U–Pb zircon geochronology of peak and retrograde stages of ultrahigh-pressure metamorphic rocks from the Kokchetav massif, northern Kazakhstan: Earth and Planetary Science Letters, v. 188, p. 185–198.

Keverne, R., 1991, Jade: New York, NY, Van Nostrand Reinhold, 376 p.

Kim, S. J., Lee, D. J., and Chang, S., 1986, A mineralogical and gemological characterization of the Korean jade from Chuncheon, Korea: Journal of the Geological Society of Korea, v. 22, no. 3, p. 278–288.

Kobayashi, S., Miyake, H., and Shoji, T., 1987, A jadeite rock from Oosa-cho, Okayma Prefecture, southwestern Japan: Mineralogical Journal, v. 13, no. 6, p. 314–327.

Komatsu, M., 1987, Hida "Gaien" belt and Joetsu belt, *in* Ichikawa, K., Mizutani, S., Hara, I., Hada, S., and Yagi, A., eds., Pre-Cretaceous terranes of Japan, IGCP project No. 224: Osaka, Japan, Nippon Insatsu Shuppan Co., Ltd., p. 25–40.

Kovalenko, I. V., and Sviridenko, A. F., 1981, Tectonic conditions for the formation of the jadeite fields of the Balkhash Region and the Polar Urals: Vestnik Moskovskogo Universiteta, Geologiya, v. 36, p. 52–59 (in Russian).

Kunz, G. F., 1906, The Bishop Collection. Investigations and studies in jade: New York, NY, Devinne Press, 2 vols.

Lacroix, A., 1930, La jadeite de Birmanie: Les roches qu'elle constitue ou qui l'accompagnent. Composition et origine: Bulletin de la Société Français de Minéralogie et Cristalographie, v. 53, p. 216–264.

Leaming, S. F., 1978, Jade in Canada: Geological Survey of Canada Papers, v. 78-19, 1–59.

Lichtner, P. C., Oelkers, E. H., and Helgeson, H. C., 1986, Interdiffusion with multiple precipitation/dissolution

reactions; transient model and steady-state limit: Geochimica et Cosmochimica Acta, v. 50, p. 1951–1966.

Loney, R. A., and Himmelberg, G. R., 1985, Ophiolitic ultramafic rocks of the Jade Mountains–Cosmos Hills area, southwestern Brooks Range, *in* The United States Geological Survey in Alaska: Reston, VA, U. S. Geol Survey Circular, p. 13–15.

Madson, M. E., 1978, Nephrite occurrences in the Granite Mountains region of Wyoming, in Boyd, R. G., Boberg, W. W., and Olson, G. M., eds., Resources of the Wind River Basin. Guidebook: Casper, Wyoming Geological Association, v. 30, p. 393–397.

Manning, C. E., 1998, Fluid composition at the blueschist-eclogite transition in the model system Na_2O-MgO-Al_2O_3-SiO_2-H_2O-HCl: Schweizerische Mineralogische und Petrographische Mitteilungen, v. 78, no. 2, p. 225–242.

McBirney, A. R., Aoki, K.-I., and Bass, M., 1967, Eclogites and jadeite from the Motagua fault zone, Guatemala: American Mineralogist, v. 52, p. 908–918.

Mével, C., and Kiénast, J. R., 1986, Jadeite-kosmochlor solid solution and chromian sodic amphiboles in jadeitites and associated rocks from Tawmaw (Burma): Bulletin de Minéralogie, v. 109, p. 617–633.

Miyajima, H., Matsubara, S., Miyawaki, R., Yokoyama, K., and Hirokawa, K., 2001, Rengeite, $Sr_4ZrTi_4Si_4O_{22}$, a new mineral, the Sr-Zr analogue of perrierite from the Itoigawa-Ohmi district, Niigata Prefecture, central Japan: Mineralogical Magazine, v. 65, no. 111–120.

Miyajima, H., Matsubara, S., Miyawaki, R., and Ito, K., 1999, Itoigawaite, a new mineral, the Sr analogue of lawsonite, in jadeitite from the Itoigawa-Ohmi district, central Japan: Mineralogical Magazine, v. 63, p. 909–916.

Miyajima, H., Miyawaki, R., and Ito, K., 2002, Matsubaraite, $Sr_4Ti_5(Si_2O_7)_2O_8$, a new mineral, the Sr-Ti analogue of perrierite in jadeitite from the Itoigawa-Ohmi District, Niigata Prefecture, Japan: European Journal of Mineralogy, v. 14, no. 6, p. 1119–1128.

Morkovkina, V. F., 1960, Jadeitites in the hyperbasites of the Polar Urals: Izvestiya Akademia Nauk SSSR, seriya geologicheskaya, no. 4, p. 78–82 (in Russian).

Moskaleva, V. N., 1962, Towards the mineralogy of the PreBalkash Jadeitites: Zapiski Vserossiyskogo Mineralogicheskogo Obshchestva, v. 91, no. 1, p. 38–49 (in Russian).

Noetling, F., 1893, Note on the occurrence of jadeite in Upper Burma: Records of the Geological Survey of India, v. 26, no. 1, p. 26–31.

Noetling, F., 1896, Über das Vorkommen von Jadeit in Ober-Birma: Neues Jahrbuch für Mineralogie, v. 1, p. 1–17.

Noh, J. H., Yu, J.-Y., and Choi, J. B., 1993, Genesis of nephrite and associated calc-silicate minerals in the Chuncheon area: Journal of the Geological Society of Korea, v. 29, p. 199–224 (in Korean).

O'Hanley, D. S., 1996, Serpentinites, recorders of tectonic and petrological history: Oxford Monographs in Geology and Geophysics, v. 34, 256 p.

Okay, A. I., 1997, Jadeite—K-feldspar rocks and jadeitites from northwest Turkey: Mineralogical Magazine, v. 61, p. 835–843.

Okay, A. I., 2002, Jadeite–chloritoid–glaucophane–lawsonite blueschists in northwest Turkey: Unusually high P/T ratios in continental crust: Journal of Metamorphic Geology, v. 20, p. 757–768.

Okay, A. I., and Kelly, S. P., 1994, Tectonic setting, petrology, and geochronology of jadeite + glaucophane schists from northwest Turkey: Journal of Metamorphic Geology, v. 12, p. 455–466.

Ou Yang, C. M., 1984, Terrestrial source of ureyite: American Mineralogist, v. 69, p. 1180–1183.

Ou Yang, C. M., 2001, Characteristics of violet jadeite jade and its coloration mechanism: Baoshi He Baoshixue Zazhi, v. 3, no. 1, p. 1–6.

Peacock, S. M., 1987, Serpentinization and infiltration metasomatism of the Trinity peridotite, Klamath province, northern California: Implications for subduction zones: Contributions to Mineralogy and Petrology, v. 95, p. 55–70.

Peacock, S. M., 1993, The importance of blueschist → eclogite dehydration reactions in subducting oceanic crust: Geological Society of America Bulletin, v. 105, p. 684–694.

Prokhor, S. A., 1991, The genesis of nephrite and emplacement of the nephrite-bearing ultramafic complexes of East Sayan: International Geology Review, v. 33, p. 290–300.

Protod-yakonova, Z. M. and Mansurov, M., 1973, Tremolite nephrite as an effect of dolomite wallrock alteration in the Kansay ore field, Kuraminskiy Mountains: Uzbekskiy geologicheskiy zhurnal, v. 1, p. 20–22 (in Russian)

Rawson, J., 1995, Chinese jade from the neolithic to the Qing. London, UK: British Museum Press, 463 p.

Schmidt, M. W., and Poli, S., 1998, Experimentally based water budgets for dehydrating slabs and consequences for arc magma generation: Earth and Planetary Science Letters, v. 163, nos. 1-4, p. 361–379.

Sedqui, A., and Guy, B., 2001, Échange chromatographique de deux constituents indépendents entre un fluide aqueux et une solution solide à trois poles; application à la substitution Ca-Fe-Mn des grenats de skarn: Comptes Rendus de l'Academie des Sciences, Serie II, Science de la Terre et des Planetes, v. 332, no. 4, p. 227–234.

Seitz, R., Harlow, G. E., Sisson, V. B., and Taube, K. A., 2001, "Olmec Blue" and formative jade sources: New discoveries in Guatemala: Antiquity, v. 87, p. 687–688.

Sekerin, A. P., Men-shagin, Yu. V., Lashchenov, V. A., Sekerina, N. V., 1998, New ophiolitic belt in eastern Sayan:

Byulleten' Moskovskogo Obshchestva Ispytateley Prirody, Otdel Geologicheskiy, v. 73, no. 1, p. 12–16.

Sekerin, A. P., and Sekerina, N. V., 1986, Genesis of leucocratic nephrites of the central Vitim Highlands: Doklady Akademii Nauk SSSR, v. 284, no. 1, p. 103–105.

Sekerin, A. P., Sekerina, N. V., Men-shagin, Yu. V., and Lashchenov, V. A., 1997, Principles for prediction of nephrite deposits: Otechestvennaya Geologiya, v. 1997, no. 5, p. 42–46 (in Russian).

Sekerina, N. V., 1992, Main regularities of nephrite formation: Russian Geology and Geophysics, v. 33, no. 4, p. 31–36.

Sherer, R. L., 1972, Geology of the Sage Creek nephrite deposit, Wyoming: Contributions to Geology (University of Wyoming), v. 11, no. 2, p. 83–86.

Shi, G. H., Cui, W. Y., and Liou, J., 2001, The petrology of jadeite-bearing serpentinized peridotite and its country rocks from Northwestern Myanmar (Burma): Acta Petrologica Sinica, v. 17, p. 483–490.

Shi, G. H., Cui, W. Y, Tropper, P., Wang, C. Q., Shu, G.-M., and Yu, H., 2003, The petrology of a complex sodic and sodic-calcic amphibole association and its implications for the metasomatic processes in the jadeitite area in northwestern Myanmar, formerly Burma: Contributions to Mineralogy and Petrology, v. 145, p. 355–376.

Shidô, F., 1958, Calciferous amphibole rich in sodium from jadeite-bearing albitite of Kotaki, Niigata Prefecture: Journal of the Geological Society of Japan, v. 64, p. 595–600.

Silva, Z. C. G., da, 1967, Studies on jadeites and albites from Guatemala: Unpubl. M.A. dissertation, Rice University, Houston, Texas, 32 p.

Silva, Z. C. G., da, 1970, Origin of albitites from eastern Guatemala: Bolletin dos Servicos de Geologia e Minas (Brazil), no. 22, p. 23–32.

Sisson, V. B., Harlow, G. E., Sorensen, S. S., Brueckner, H. K., Sahm, E., Hemming, S., and Avé Lallemant, H. G., 2003, Lawsonite eclogite and other high-pressure assemblages in the southern Motagua Fault zone, Guatemala: Implications for Chortís collision and subduction zones [abs.]: Geological Society of America Abstracts with Program, v. 35, no. 6 (abstract 61863, CD-ROM 260-36).

Smith, D. C., and Gendron, F., 1997, New locality and a new kind of jadeite jade from Guatemala; rutile-quartz-jadeitite [abs]: Terra Abstracts, v. 9, suppl. 1, p. 35.

Sorensen, S. S., and Barton, M. D., 1987, Metasomatism and partial melting in a subduction complex: Catalina Schist, southern California: Geology, v. 15, p. 115–118.

Sorensen, S. S., and Harlow, G. E., 1998, A cathodoluminescence (CL)-guided ion and electron microprobe tour of jadeitite chemistry and petrogenesis [abs.]: Geological Society of America Abstracts with Program, v. 30, p. A-60.

Sorensen, S. S., and Harlow, G. E., 1999, The geochemical evolution of jadeitite-depositing fluids [abs.]: Geological Society of America Abstracts with Program, v. 31, p. A-101.

Sorensen, S. S., and Harlow, G. E., 2001, The jadeitites of Nansibon, Myanmar: Records of the geochemistry of subduction zone fluids [abs.]: Eleventh Annual V. M. Goldschmidt Conf., Abs. #3800, Houston, Lunar and Planetary Institute, LPI Contrib. No. 1088, (CD-ROM).

Sorensen, S. S., Harlow, G. E., and Rumble, D., III, 2003, SIMS oxygen isotope analyses of jadeitite: Trace element correlations, fluid compositions, and temperature estimates [abs.]: Geological Society of America Abstracts with Program, v. 35, no. 6 (abstract #225; CD-ROM, 90-7).

Suturin, A. N., 1988, Physicochemical model of nephritization: Doklady, USSR Academy of Sciences, Earth Science Section, v. 291, p. 199–201.

Suturin, A. N., and Zamaletdinov, R. S., 1984, Nephrites: Novosibirsk, Nauka Press (in Russian).

Tan, L-P., Lee, C. W., Chen, C-C., Tien, P-L., Tsui, P-C., and Yui, T-F., 1977, A mineralogical study of the Fengtian nephrite deposits of Hualien, Taiwan: National Science Council Special Publication No. 1, 81 p.

Tang Yanling, Chen Baozhang, and Jiang Reng, 1994, Zhongguo Hetian Yu (Hetian jade of China): Xinjiang People's Publishing House, 353 p.

Thin, N., 1985, Petrologic-tectonic environment of jade deposits, Phankant-Tawmaw Jade Tract: Rangoon, Burma, Burma University, 30 p.

Tsien, H. H., Lo, H.-J., and Lin, S-B, 1996a, Crystal growth and whitening of archaic tremolite yu: Acta Geologica Taiwanica, v. 32, p. 131–147.

Tsien, H. H., Tan, L.-P., and Douglas, J.G., 1996b, Geology of tremolitic rock and petrofabrics of archaic Chinese yu: Acta Geologica Taiwanica, v. 32, p. 85–101.

Tsujimori, T., 2002, Phlogopite in jadeitite from the Osayama serpentinite mélange, Chugoku Mountains, southwest Japan: Bulletin of the Research Institute of Natural Science, Okayama University, v. 28, p. 25–30.

Tsujimori, T., and Itaya, T., 1999, Blueschist-facies metamorphism during Paleozoic orogeny in southwestern Japan: Phengite K-Ar ages of blueschist-facies tectonic blocks in a serpentinite melange beneath Early Paleozoic Oeyama ophiolite: Island Arc, v. 8, p. 190–205.

Turner, F. J., 1935, Geological investigations of the nephrites, serpentinites and related greenstones used by the Maoris of Otago and South Canterbury: Transactions of the Royal Society of New Zealand, v. 65, p. 187–210.

United Nations, 1979, Geological mapping and geochemical exploration in Mansi-Manhton, Indaw-Tigyaing, Kyindwe-Longyi, Patchaung-Yane and Yezin Areas,

Burma: Mineral Exploration Burma, Technical Report 7, U.N. Development Programme, 13 p.

Veblen, D. R., and Wyllie, A. G., 1993, Mineralogy of amphiboles and 1:1 layer silicates, *in* Guthrie, G. D., Jr., and Mossman, B. T., eds., Health effects of mineral dusts: Reviews in Mineralogy, v. 28, p. 61–137.

Visser, J. M., 1946, Nephrite and chrysoprase of Silesia: Mineralogist (Portland, Oregon Agate and Mineral Society), v. 14, p. 460–462.

Wang, S-Q., Duan, T-Y., and Zheng, Z-S., 2002, Mineralogical and petrological characteristics of Xiyuan nephrite and its minerogenetic model: Acta Petrologica Mineralogica (Sinica), v. 21, suppl. (Sept., 2002), p. 79–90 (in Chinese).

Wang, W.-S., 1987, Nephrite deposits of Taiwan [abs]: Pacific Rim Congress 87, Parkville, Victoria, Australasian Institute of Mining and Metallurgy, p. 639–640.

Ward, F., 2001, Jade: Bethesda, MD, Gem Book Publishers, 64 p.

Webster, R., 1975, Gems: Their sources, descriptions, and identification, third ed.: Hamden, CT, Archon Books, Shoestring Press, Inc., 931 p.

Wen, G., 2001, Ancient Chinese jade and the jade age (translation from Zhongguo guyu yuqi shidai by E. Childs-Johnson), in Childs-Johnson, E., ed., Enduring art of Jade Age China: Chinese jades of late Neolithic through Han periods: New York, NY, Throckmorton Fine Art, p. 31–34.

Wen, G., and Jing, Z., 1993, A geoarchaeological study of the jades from the Fengxi site of Western Zhou dynasty—geoarchaeological study of ancient Chinese jade (III): Acta Archaeologica Sinica, no. 2, p. 251–280.

Wen, G., and Jing, Z., 1996, Mineralogical studies of Chinese archaic jade: Acta Geologica Taiwanica, v. 32, p. 55–83.

Wu, R-H., Zhang, X-H., and Li, W-W., 2002, Petrological characteristics of Hetian jade in Xinjiang and nephrite from Baikal area in Russia: Acta Petrologica et Mineralogica (Sinica), v. 21, suppl. (Sept. 2002), p. 134–142.

Yui, T-F., and Kwon, S-T., 2002, Origin of a dolomite-related jade deposit at Chuncheon, Korea: Economic Geology, v. 97, p. 593–601.

Yui, T-F., Yeh, H-W., and Lee, C. W., 1988, Stable isotope studies of nephrite deposits from Fengtian, Taiwan: Geochimica et Cosmochimica Acta, v. 52, p. 593–602.

Yui, T-F., Yeh, H-W., and Lee, C. W. 1990, A stable isotope study of serpentinization in the Fengtien ophiolite, Taiwan: Geochimica et Cosmochimica Acta, v. 54, p. 1417–1426.

Zhang, L., 2002a, A study of the composition and properties of Xiuyan jade in Liaoning Province: Acta Mineralogica Sinica, v. 22, no. 2, p. 137–142 (in Chinese).

Zhang, L., 2002b, Characteristics and quality of Xiyuan jade in Liaoning Province: Acta Petrologica et Mineralogica (Sinica), v. 21, suppl. (Sept. 2002), p. 134–142 (in Chinese).

Zhong, H., 1995, The discovery of Meiling jade in southern Liyang, Jiangsu: Jiangsu Geology, v. 19, no. 3, p. 176–178.

Zoltai, T., 1981, Amphibole asbestos mineralogy, *in* Veblen, D. R., ed., Amphiboles and other hydrous pyriboles: Reviews in Mineralogy, v. 9A, p. 237–238.